712528

UNCLASSIFIED

HW 18258

DEVELOPMENT DIVISION
HEALTH INSTRUMENT DIVISIONS

COUNTER CALIBRATIONS IN THE H. I. METHODS GROUP

July 1, 1950

REPOSITORY PNL
COLLECTION I-131 Atmosphere
BOX No. N/A
FOLDER N/A

INVENTORIED
JUN 24 1992
DOCUMENT AUDIT AND INVENTORY UNIT

INVENTORIED
1953
DOCUMENT AUDIT AND INVENTORY UNIT

GENERAL ELECTRIC
NUCLEONICS DEPARTMENT

HANFORD WORKS

RICHLAND, WASHINGTON

UNCLASSIFIED

THIS DOCUMENT IS PUBLICLY AVAILABLE

1083722

UNCLASSIFIED

HW-18258
Health and Biology

This document consists
of 53 pages Copy No. 8
of 159 Copies. Series A

COUNTER CALIBRATIONS IN THE HEALTH INSTRUMENT METHODS GROUP

by

J. W. HEALY, L. C. SCHWENDIMAN,

R. C. THORBURN

HEALTH INSTRUMENT DEVELOPMENT DIVISION

July 1, 1950

HANFORD WORKS
RICHLAND, WASHINGTON

Operated for the Atomic Energy Commission
by the
General Electric Company

under

Contract No. W-31-109-eng-52

UNCLASSIFIED

1083723

COPY NO.	INTERNAL DISTRIBUTION
1	H. M. Parker
2	A. B. Greninger
3	C. C. Gamertsfelder
4	F. Albaugh
5	H. Schmidt
6	C. M. Patterson
7	W. A. McAdams
8	A. R. Keene
9	H. A.Kornberg - R. F. Foster
10	Z. E. Carey
11	H. J. Paas
12	D. L. Reid
13	W. Singlevich
14	R. C. Thorburn
15	J. W. Healy
16	L. C. Schwendiman
17-18	George Brown
19	Pink File
20	Yellow File
21	700 File
22 - 23	Extra
24	300 File

1083724

COPY NUMBER	EXTERNAL DISTRIBUTION
25 - 32	Argonne National Laboratory
33	Armed Forces Special Weapons Project
34 - 35	Atomic Energy Commission - Washington
36	Battelle Memorial Institute
37	Brush Beryllium Company
38 - 41	Brookhaven National Laboratory
42	Bureau of Medicine and Surgery
43	Bureau of Ships
44	California Institute of Technology (Robert F. Bacher)
45 - 48	Carbide and Carbon Chemicals Division (K-25 Plant)
49 - 52	Carbide and Carbon Chemicals Division (Y-12 Plant)
53	Chicago Operations Office
54	Columbia University (J. R. Dunning)
55	Columbia University (G. Failla)
56	Dow Chemical Company
57	H. K. Ferguson Company
58	Harshaw Chemical Corporation
59	Idaho Operations Office
60 - 61	Iowa State College
62	Kansas City Operations Branch
63 - 64	Kellex Corporation
65 - 68	Knolls Atomic Power Laboratory
69 - 71	Los Alamos Scientific Laboratory
72	Mallinckrodt Chemical Works
73	Massachusetts Institute of Technology (A. Gaudin)
74	Massachusetts Institute of Technology (A. R. Kaufmann)
75 -77	Mound Laboratory
78	National Advisory Committee for Aeronautics
79 - 81	National Bureau of Standards
82 - 83	Naval Radiological Defense Laboratory
84	Naval Medical Research Institute
85	New Brunswick Laboratory
86 - 88	New York Operations Office
89	North American Aviation, Inc.
90 - 97	Oak Ridge National Laboratory
98	Patent Branch (Washington)
99	RAND Corporation
100	Sandia Corporation
101 - 102	Santa Fe Operations Office
103	Sylvania Electric Products, Inc.
104 - 118	Technical Information Division (Oak Ridge)
119	USAF, Air Surgeon (Lt. Col. R. H. Blount)
120	USAF, Armament Division
121 - 122	USAF, Director of Research and Development (Col. R. J. Mason, Fred W. Bruner)
123	USAF, Eglin Air Force Base (Major A. C. Field)
124	USAF, Kirtland Air Force Base (Col. Marcus F. Cooper)
125	USAF, Maxwell Air Force Base (Col. F. N. Moyers)
126 - 127	USAF, NEPA Office

1083725

External Distribution (Continued)

128 - 129	USAF, Office of Atomic Energy (Col. H. C. Donelly, A. A. Fickel)
130	USAF, Offutt Air Force Base (Col. H. R. Sullivan, Jr.)
131	USAF, Wright-Patterson Air Force Base Rodney Nudenberg)
132	U. S. Army, Atomic Energy Branch (Lt. Col. A. W. Betts)
133	U.S. Army, Army Field Forces (Captain James Kerr)
134	U.S. Army, Commanding General, Chemical Corps Technical Command (Col. John A. MacLaughlin thru Mrs. Georgia S. Benjamin)
135	U.S. Army, Chief of Ordinance (Lt. Col. A R. Del Campo)
136	U S. Army, Commanding Officer, Watertown Arsenal (Col. Carroll H. Deitrick)
137	U.S Army, Director of Operations Research (Dr. Ellis Johnson)
138	U S. Army, Office of Engineers (Allen O'Leary)
139	U.S. Army, Office of the Chief Signal Officer (Curtis T. Clayton thru Maj. George C. Hunt)
140	U.S. Army, Office of the Surgeon General (Col. W. S. Stone)
141 - 142	U. S. Geological Survey (T.B Nolan)
143	USAF, Director of Plans and Operations (Col. R. L. Applegate)
144	U.S. Public Health Service
145	University of California at Los Angeles
146 - 150	University of California Radiation Laboratory
151 - 152	University of Rochester
153	University of Washington
154 - 155	Western Reserve University
156 - 159	Westinghouse Electric Company

1083726

COUNTER CALIBRATIONS IN THE H.I. METHODS GROUP

INTRODUCTION:

One of the chief limitations in the application of radiochemistry to quantitative techniques, is the lack of accurate methods for measuring the exact quantities of the radiations involved and then interpreting these measurements in terms of the amount of active material. Measurements have been either relative or with large uncertainties in the final value with poor cross-checks between various laboratories.[1] A considerable body of information has been published in the last few years concerning the effect of backscatter [2] [3] [4], self-absorption,[5] [6] and coincidence losses[7]. The applications of these techniques and data to any given problem are sometimes difficult particularly when a large number of different isotopes are measured by the same laboratory force.

The Methods Section of the Health Instrument's Development Division has been faced with the necessity of making measurements of most fission products and a large number of active isotopes produced by pile irradiation. The original sample may be vegetation, water, filter paper, oil, dirt, or any of the other numerous media in which active materials could be found. The following work is the result of studies made during the past two years with the ultimate objective of providing methods for measuring accurately the activity of a "spike" solution which may then be used to evaluate the overall yield of the analysis, including the laboratory manipulations and the counting efficiencies.

This paper is presented to describe the techniques developed and some of the factors measured. Estimates of the accuracy available with these techniques and checks between methods are included.

SUMMARY:

Parallel plate pulse counters are used for measuring the alpha emission of samples. A geometry of 52% for a point source is accepted for these units.

1083727

A correction factor of 0.913 is applied to a 1-1/2" sample spread by ordinary laboratory techniques. Coincidence losses have been determined as 2% per 1000 counts per minute.

Beta counting is carried out on end window counters with 2-4.5 mg/cm^2 mica windows 1-1/8" in diameter. Shielding and shelf arrangements for sample mounting are detailed. Methods to determine the various correction factors and tabular data are presented. Backscatter corrections for radio-isotopes of C, S, Co, I, RaE, Rh, Cs, Y, Ce, and P on various backing materials range from 5% to 74%. Absorption losses in the air and window are determined by extrapolation of an absorption curve. Tables of experimental slopes of the absorption curve for a number of isotopes enable such an extrapolation with no further measurements. Corrections for an extended source are made in terms of the point source geometry by measuring the variation of geometry across the face of the tube and integrating over the area of the source. The measured variations in geometry for points off the axis of the tube are confirmed by theoretical calculations. The net geometry of the tube is calculated from the known disintegration rate of the source and the measured correction factors for the beta counting. Agreement well within 5% on 16 beta counters is obtained between a Bureau of Standards calibrated RaE source and RaE sources prepared in this laboratory. Calculated geometry values do not agree with the measured values presumably due to a non-active volume immediately inside of the flange supporting the counter window. Self-absorption curves for several isotopes with most common precipitates are presented. An apparent difference in the disintegration rate of a uranium chip when counted at various distances from the tube is resolved by self-absorption considerations. Gamma corrections are determined, when required, by counting the source through an aluminum absorber thick enough to absorb all beta particles. Coincidence losses are accepted as 0.2% per 1000 counts per minute.

1083728

EQUIPMENT:

A. Alpha Counters

The alpha counting equipment consists of parallel plate pulse counters known locally as the "standard" alpha counter.(8) The chamber is mounted in a brass tube 4" in diameter and 13" long. The lower electrode is mounted on a door which opens at the bottom of the chamber. A negative potential of 1000 volts is applied to this electrode through a pin jack in the rear of the shell when the door is closed. The upper plate is connected by a short lead to the grid of a preamplifier unit contained in the brass shell. This entire unit is suspended on a rubber shock mount to minimize microphonics.

The pulse from the preamplifier is fed to another amplifier with a gain of 100,000 and then to a Higginbotham or Offner scaler. An oscilloscope is provided on the output of the amplifier so that arc discharges, microphonics or power pulses may be detected. The amplifier is biased so that only alpha pulses and not tube noise or beta pulses are passed to the scaler.

B. Beta Counters

Mica window GM tubes filled to a pressure of ten cm. of mercury with alcohol-argon, fabricated at Hanford Works by the Instrument Division are used. The tube case is two and one-half inches long, and one and one-quarter inches outside diameter with a mica window of 2 to 4.5 mg/cm^2 cemented to a flange on the lower end of the cylinder.(9) The tube is mounted at the top of a set of aluminum shelves designed to hold sample mounting cards at known fixed distances from the counter face.(10) (Fig. 1.) The distance from the flange carrying the mica window to the first shelf is set with a gauge at 0.191 inches. The distances from the window to other shelves are: 2nd shelf, 0.816; 3rd shelf, 1.441 in; 4th shelf, 2.066 in.; 5th shelf, 2.691 in. The entire assembly is contained in a lead shield with two-inch walls to minimize background radiation from cosmic rays and activity in the counting room. The counter is operated as a self-quenched unit feeding into a scale of 64.

1083729

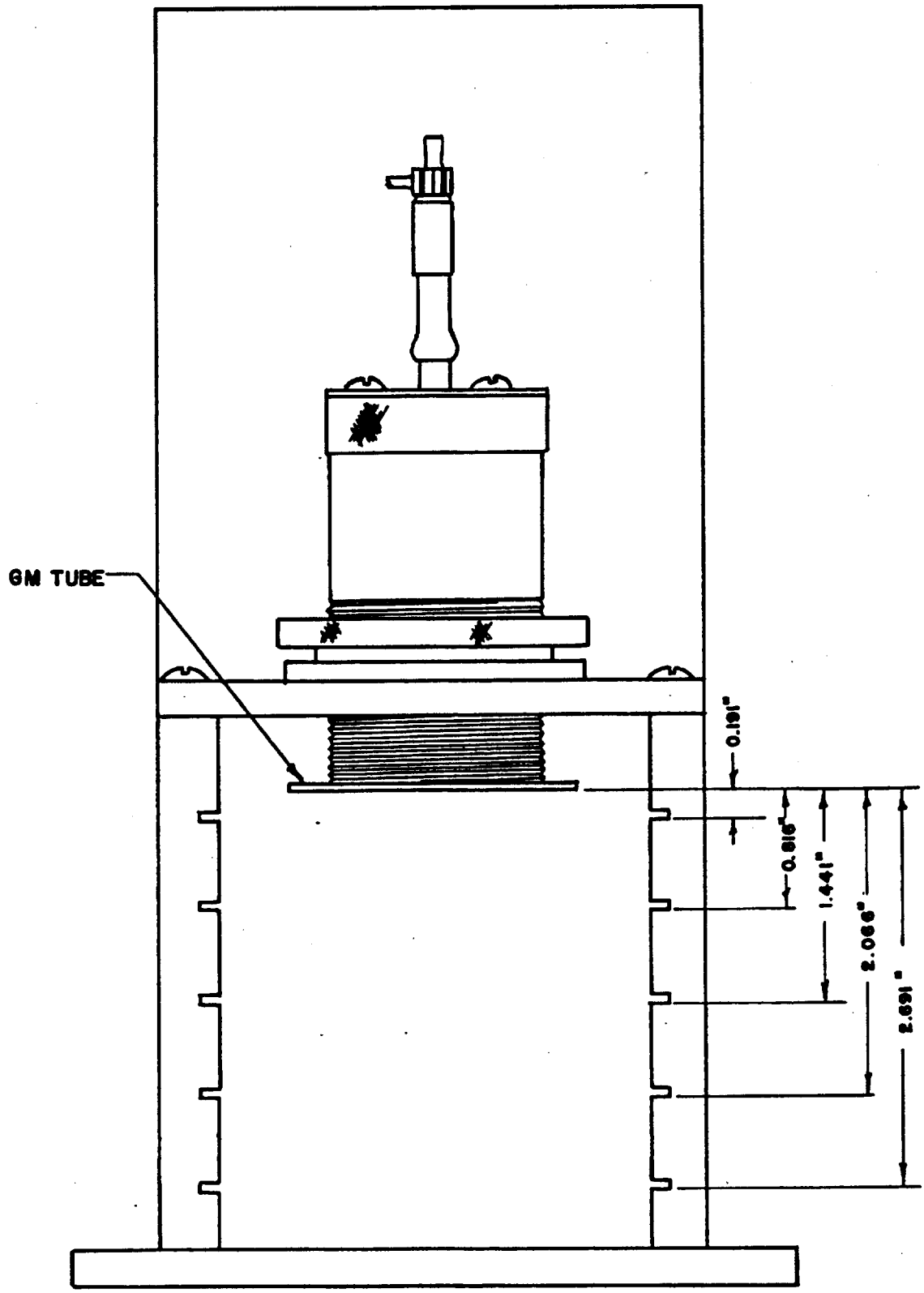

FIG. 1

END MICA WINDOW GM TUBE SUPPORT AND SHELF ASSEMBLY.

C. Counting Plates

Since the majority of the work involves low activity densities, it is necessary to use counting plates on which relatively large volumes (several ml.) may be evaporated without the loss of too much time. A small amount of work has been done with one-inch watch glasses, but these are generally unsatisfactory because of their non-uniformity and the difficulty of indexing the active surface with respect to the counter. At the present time a 1-1/2 inch diameter, 0.005 inch thick stainless steel plate as sketched in Fig. 2 is used. It has the advantage of allowing 3-4 ml. to be evaporated at one time and is easily indexed to a known position. The chief difficulty is the tendency for material to concentrate around the edge thus losing geometry, particularly in the beta counters. New plates, designed with radiused corners at the bottom have been made available to minimize this difficulty. Two sizes detailed in Fig. 3 are being used; the 1-1/2" plate for alpha counting and the 1" plate for beta.

IV. ALPHA COUNTING:

The factors involved in alpha counting are much simpler than those for beta counting. The chief difficulty, other than those inherent in the instrument such as coincidence losses, is with self-absorption since even a small amount of material on the plate will give significant losses in a 2π solid angle counter. An attempt is made to purify samples for alpha measurement to the point where losses are negligible.

A. Geometry

The geometry of the alpha counter has been accepted as 52% for thin samples mounted on platinum.[11] Although most of the samples are mounted on stainless steel (0.005 thick), this value for the geometry has still been used.

The effect of changes in sample diameter has been investigated in two ways: (1) by moving a point source across the chamber pedestal and counting at intervals, and (2) by measuring aliquots of the same solution in the form of a small diameter source and as a source spread over the area of a 1-1/2" plate. The point source

1083731

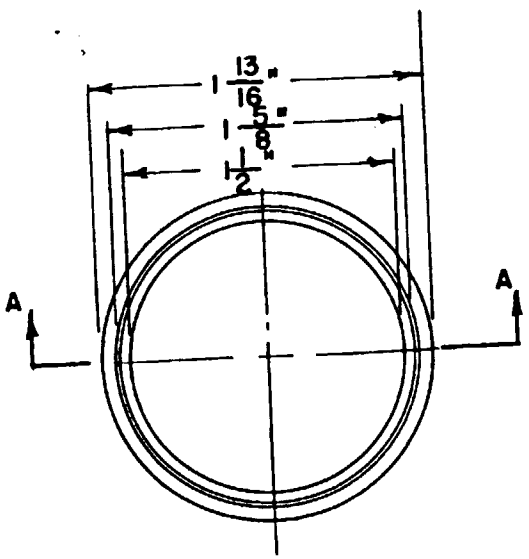

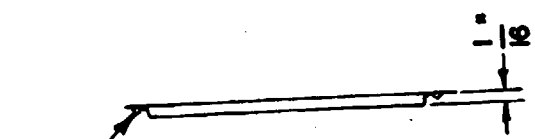

SEC. AA

PLATES WITHOUT STIFFENING BEAD HAVE ALSO BEEN USED

FIG. 2
STANDARD PLATE-EARLIER DESIGN

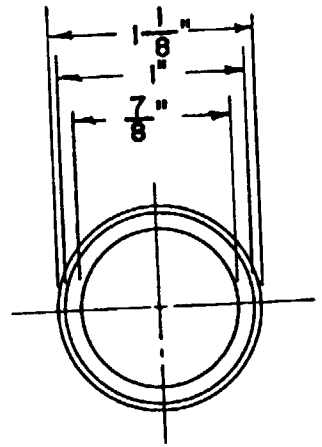

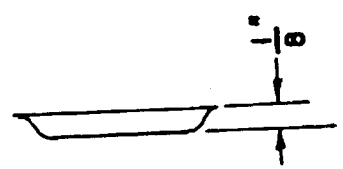

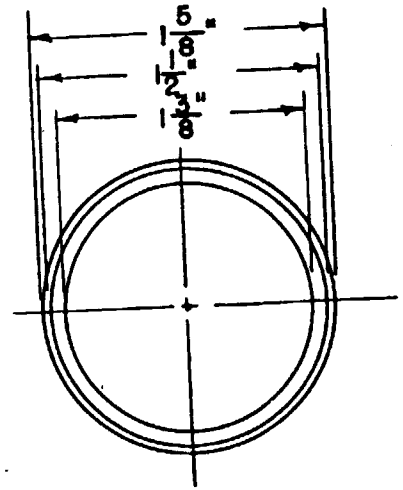

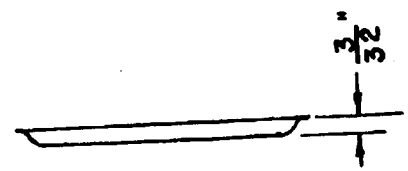

FIG.3
RECENT DESIGN PLATES

1083132

in the first method consisted of a small amount of plutonium spread over a diameter of 1/16". This source was counted at 3/16" intervals across the diameter of the pedestal and the results plotted as counting rate versus distance from the center. (Fig. 4.) This curve represents the variation across the diameter for a line source. For a circular plane source, it is necessary to account for the fact that in an annular element of area 2π rdr, near the periphery there will be a larger fraction of the material than for an annulus of equal width (dr) near the center assuming uniform distribution of the activity over the surface. This may be accounted for graphically by integrating the area under a plot of the product of the radius and the counting rate versus the radius and comparing this area to the area under the straight line that would result if there were no loss in counting rate at increased radii. This method assumes uniform distribution of the activity on the plate and a symmetrical response of the counting chamber along all diameters. Such a procedure gives a value of 0.996 for a 1-1/2" source and .925 for a 1-7/8" source. These figures represent the ratio of the number of counts measured for a uniformly spread source to the number measured for the same amount of activity as a point source in the center of the chamber.

Unfortunately it is especially difficult to realize the first assumption of uniform spread when a large number of plates are prepared by evaporation. The material tends to concentrate around the corner between the bottom of the plate and the edge, thus giving a higher loss than would be expected from the above work. Two series of ten plates were prepared, one with the activity confined to the center 1/2" diameter of the plate and the other with the activity spread by adding the "spike" solution to two ml. of water and spreading over the plate. This test gave a ratio of 0.913 with a combined standard deviation of 0.016. This figure is representative of the technique of only one operator and may vary slightly from person to person depending upon their skill and the care expended upon the sample.

There are some indications that non-reproducible results on these units may be due to differences in the geometry of the chamber at the edge of the pedestal.

1083733

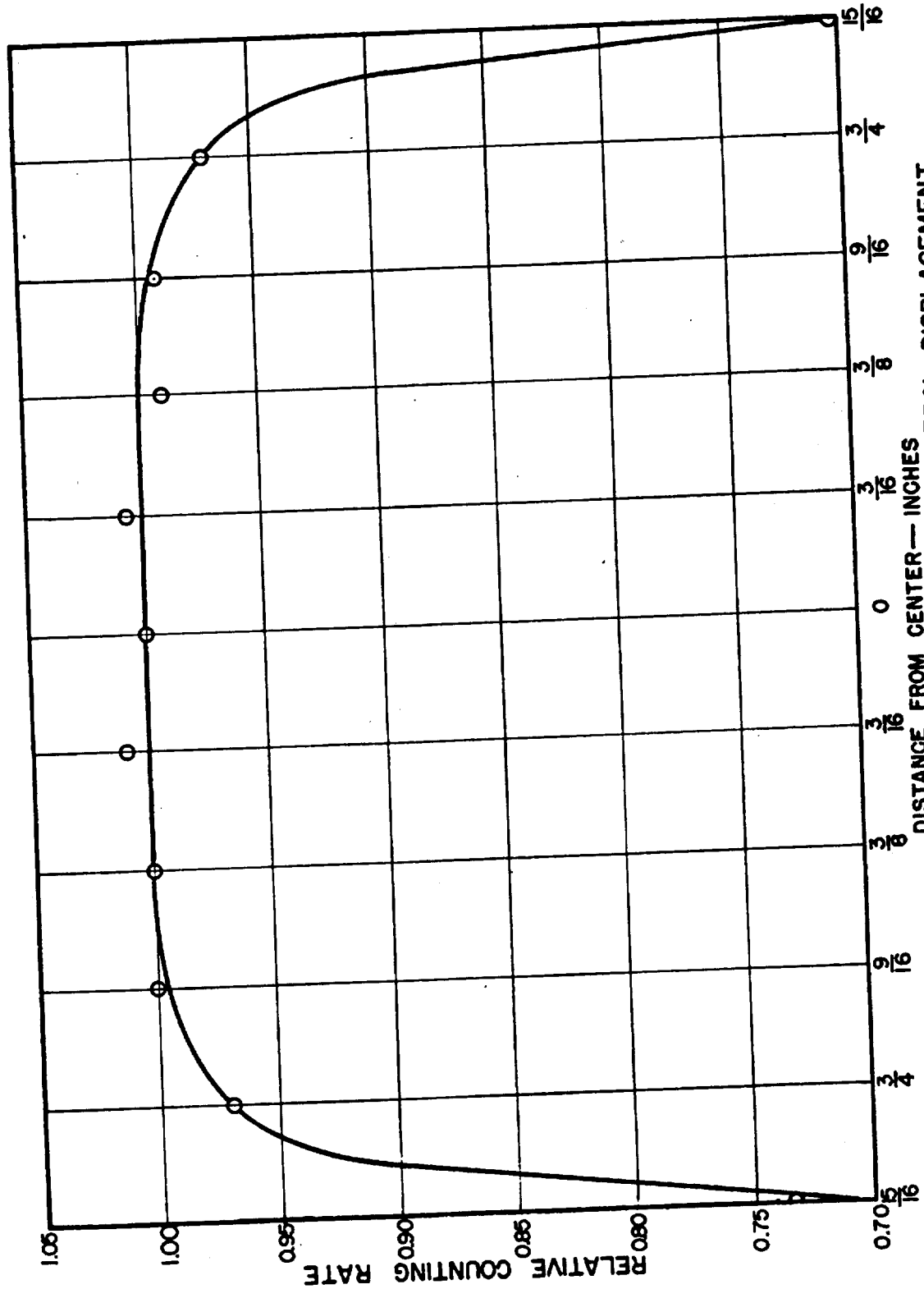

FIG. 4. VARIATION IN COUNTING RATE WITH LATERAL DISPLACEMENT OF A POINT SOURCE. STD. ALPHA CHAMBER.

1083734

Thus, one counter may be adjusted so that only a small fraction of the particles originating at the edge of the chamber will register while another counter may be adjusted so that all particles originating at the edge will register. This is particularly true if the pulse height selector and gain are adjusted with a small source at the center of the chamber. Present plans are to make such control measurements with a uniform spread source or an annular source to emphasize these edge effects.

B. Coincidence Losses

Although most of the samples measured are low level (less than 25 d/m), occasional measurements at higher levels have been needed for calibration of sources, development of procedures, etc. The value of the loss in counting rate due to coincidence (i.e. the effect of two pulses arriving within the dead time of the counter) has been quoted as 0.75% per thousand counts per minute. To determine the value of this loss with the counters used, a series of small sources of plutonium were prepared. Each source of approximately 500 c/m, was placed in a reproducible position on the pedestal and counted for a total of 50,000 counts. The sources were then counted in groups of two, three, four, etc., until thirteen sources, aggregating about 6000 c/m were measured, each located at the same point it had occupied when counted individually. (Fig. 5) The data thus obtained follows the relationship,

$$Y = X(1 + kX)$$

in which,

Y = true count

X = observed count

K = a constant (20×10^{-6})

The true count was taken to be the sum of the individual counts on the low counting sources.

On a percentage basis, the coincidence losses thus determined represent 2.0± 0.2% for each 1000 counts per minute observed. The plot in Fig. 5 can be used directly to obtain the coincidence-corrected counting rate for this unit.

1083735

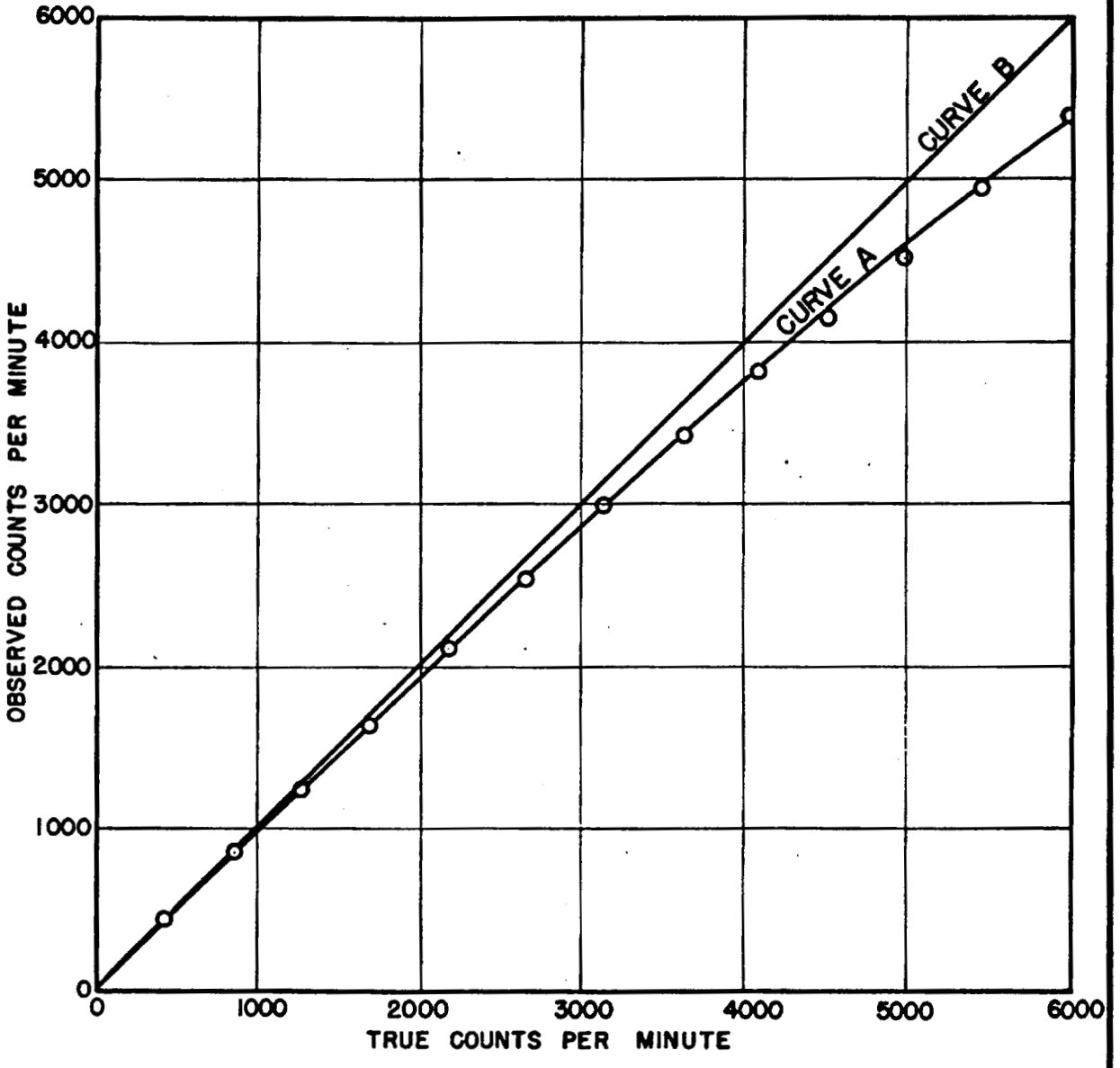

CURVE A: EXPERIMENTAL POINTS AND PLOT OF EQUATION:

TRUE C/M = OBS. C/M + K(OBS. C/M)^2 K = 20.0 X 10^{-6}

CURVE B: NO COINCIDENCE LOSS CURVE.

FIG. 5. COINCIDENCE LOSS – STD. ALPHA CHAMBER (NO. 4)

BETA COUNTING

The use of Geiger counters for beta counting requires exacting technique both in the preparation of the sample and in the measurement because of the large number of factors that will affect the results. Any program of calibration must include the control and measurement of values of correction factors for backscatter, absorption in the mica window and air above the source, changes in the geometry with sample diameter, self-absorption, and certain other factors of lesser importance.

A. Backscatter

The number of particles entering the counter from a source mounted on one of the shelves is partially a function of the number of particles scattered from the sample plate and the sides of the shield and shelf assembly. The greatest contribution arises from the sample mount itself and from any precipitate on the plate.

The amount of scatter from the plate is dependent upon the energy of the primary particle, upon the atomic number and thickness of the sample mount, and to some extent, upon the geometry of the counting since the scatter is probably not symmetrical and the probability of small angle scatter is greater than for large angle scatter.

Backscatter corrections for various isotopes mounted on several materials have been obtained by preparing point sources of the active isotopes on thin Formvar film and measuring the counting rate with and without backing material. The assembly used for this purpose is illustrated in Fig. 6.

Formvar film of thickness of 0.3 to 0.5 mg/cm^2 is stretched taut and cemented over a flat aluminum ring. A small droplet of active isotope with negligible carrier is deposited at the center where it is carefully dried under an infrared lamp. The holder (Fig. 6) is of aluminum and is provided with side tongues to fit the grooves of the shelf positions in the counter. A circular recess to

take the aluminum ring is turned in the upper surface to a shoulder which is within 0.001" of the plane of the bottom of the side tongue. The film side of the ring is thus positioned at the exact level of the shelf. The hole from the bottom accommodates a threaded ring, the upper end of which is counterbored to leave a shoulder upon which can be inserted various backing material discs. A count is made with no backing material, then the backscatter disc of interest is inserted in the ring and brought carefully just to the source film, and a second count made. The ratio of the second count to the first is the backscatter factor.

Backscatter from the 0.3 to 0.5 mg/cm^2 film is negligible as evidenced by the full backscatter curve of RaE on aluminum. Using the slope of the initial portion of the curve and extrapolating over 0.5 mg/cm^2 changes the backscatter factor by less than 1/2%.

Figure 7 illustrates the curve obtained when various thickness of aluminum are used to back a RaD-RaE source covered with 3.13 mg/cm^2 of cellophane to cut out the soft beta particles from RaD and alphas from RaF, allowing the measurement of only the 1.17 Mev particle from RaE. This curve demonstrates the general relationship between thickness of backing material and backscatter; the backscatter reaching a saturation value at about one-fifth the range of the particles in the substance. For energies below 0.6 Mev the amount of this saturation backscatter depends upon the energy. For emitters with energy greater than 0.6 Mev, the backscatter from a given material of greater than saturation thickness is practically constant. It is thus advisable to make all measurements using an arrangement to give maximum backscatter.

From Figure 7 the counting rate from a RaE source mounted on a thickness of aluminum sufficient to give saturation is 1.29 times the expected rate. Thus the corrected rate would be 1/1.29 or 77.5% of the counting rate measured with an aluminum backing.

Several isotopes and several materials have been investigated to determine the backscatter correction factors. The data obtained are presented in Table I.

1083738

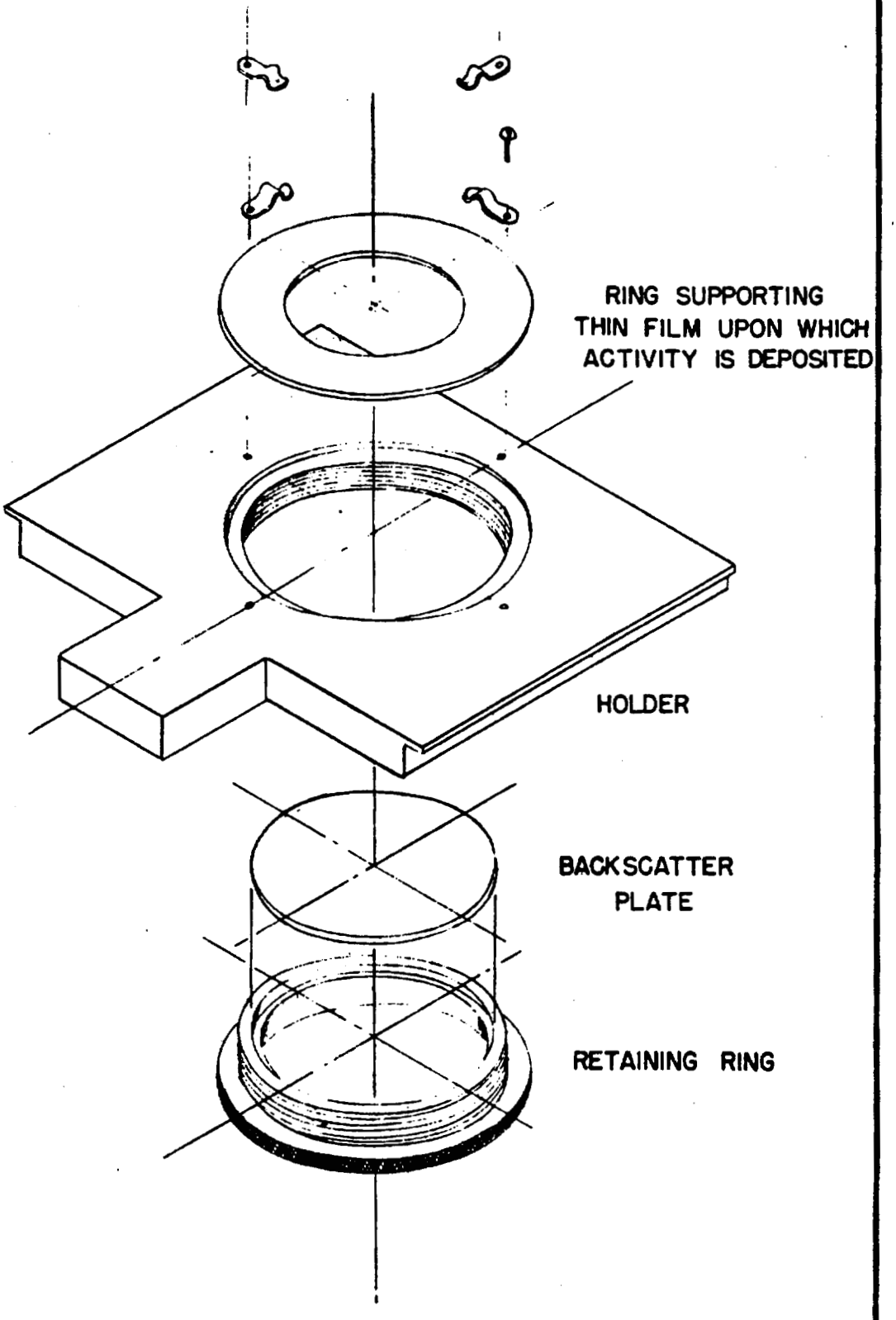

FIG. 6. ASSEMBLY USED FOR EVALUATING BACKSCATTER

1083739

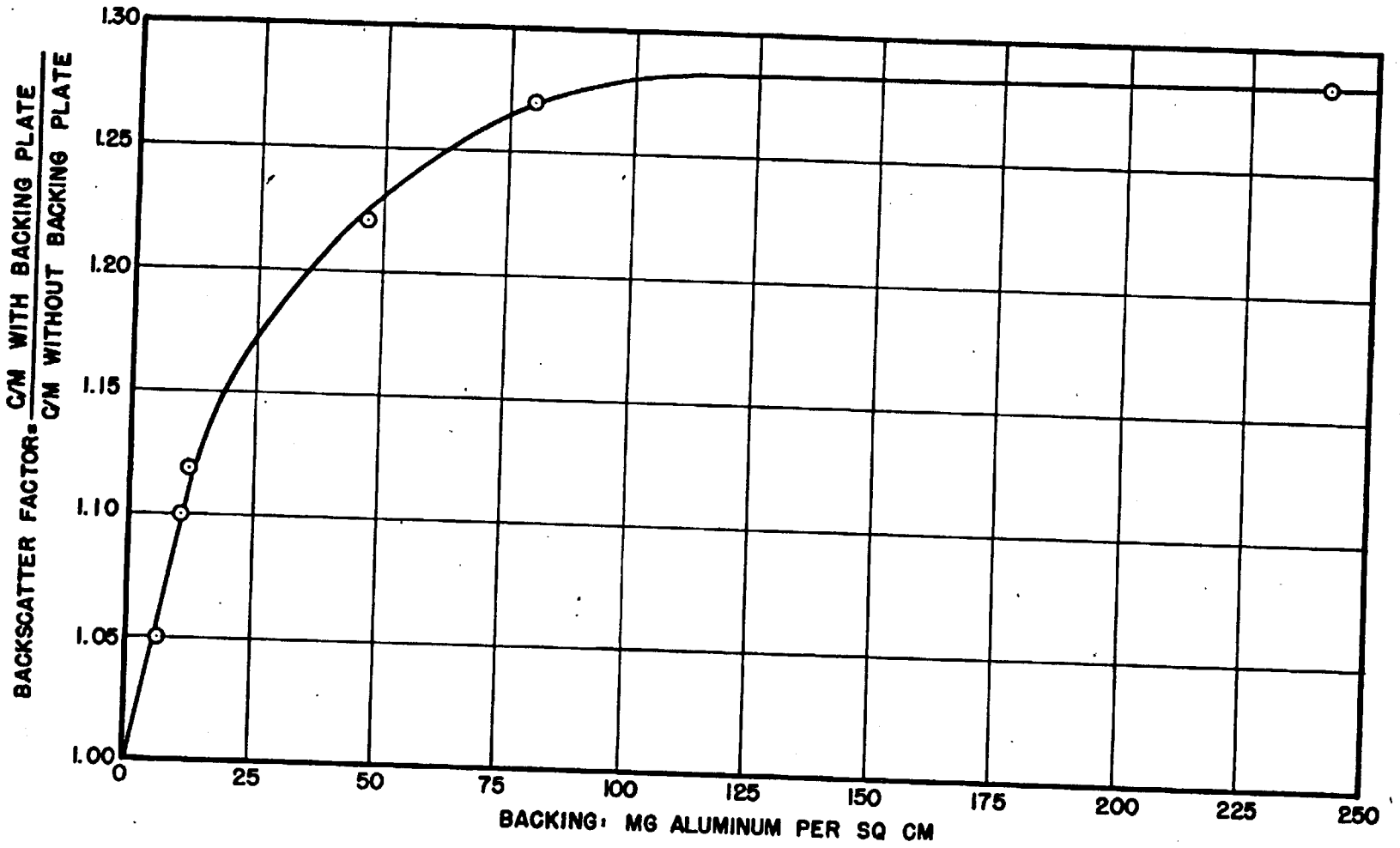

FIG. 7. BACKSCATTER OF RADIUM E (1.17 MEV) BETA PARTICLES FROM ALUMINUM

1083140

Table 1

BACKSCATTER CORRECTIONS FOR THE FIRST SHELF (APPROX. 23% GEOMETRY)

Isotope	Beta Energy Mev	BACKING MATERIAL						
		1" Watch Glass	Aluminum (Max. Thickness)	.004" Stainless Steel 87 mg/cm^2	Silver		Platinum	
					127 mg/cm^2	254 mg/cm^2	128 mg/cm^2	247 mg/cm^2
C^{14}	0.15	1.02	1.03	1.05	1.12	1.17	1.16	1.18
S^{35}	0.17	1.05	1.07	1.11	1.17	1.18	1.27	1.26
Co^{60}	0.3	1.14	1.17	1.26	1.48		1.63	
I^{131}	0.6 & 0.25	1.18	1.19	1.26	1.42		1.58	
Cs^{137}	0.5 & 0.8	1.21	1.26	1.33	1.61		1.74	
RaE	1.17	1.23	1.29	1.41	1.58	1.60	1.74	
P^{32}	1.7	1.25	1.29	1.38			1.61	
Ce^{144} Pr^{144}	0.35 & 3.0	1.22	1.27	1.27	1.58	1.66		
Ru^{106} Rh^{106}	0.03 & 3.9	1.23	1.30	1.26	1.47	1.56	1.63	1.74

The dependence of backscatter on atomic number is readily apparent from this data. The estimated accuracy of the factor is about ± 0.03.

1083741

B. Absorption in Air and Counter Window

Since beta particles are emitted in a continuous spectrum with a significant number at the low energy end of the spectrum, some of the electrons will not have sufficient energy to penetrate the window to the sensitive volume of the counter. Still others will be scattered out of the direct beam by the air or mica window and will not be recorded. If a true value is to be assigned to the disintegration rate of the source, the loss due to these two factors must be measured.

The first portion of a beta particle absorption curve follows very closely an exponential relation. Thus a plot on semi-logarithmic paper of counting rate versus absorber thickness should give a straight line for thin absorbers. This curve may then be extrapolated through the thickness equivalent to the window and air present.

Unfortunately, the slope of this line is dependent upon the relative geometries of the source, the counter, and the absorber. If, for instance, a thin absorber is placed directly upon the source, an increase in the counting rate may be noted because of scatter from portions of the absorber outside of the cone of primary particles. An ideal absorption measurement would use an absorber no larger in size than the circular area of the intersection of the absorber and the cone of primary particles entering the counter. Placing the absorbers as near to the window as possible essentially realizes the ideal position. In this position the extremities of the absorber cannot scatter betas into the window, and losses by scatter are minimized. The scatter from the mica window itself would be more exactly evaluated, since with the absorbers close to the window, they will effectively act as an increased window thickness. Whatever placement is made will be in error to some extent because of the scatter occurring in the air. This, of course will be minimized with the sample on the first shelf because of the small distance (0.191") between source and window.

For sources supported on the first shelf, absorbers are held at about 1/16"

1083742

from the window. For the other shelves, absorbers are placed on the first shelf.

The absorbers consist of thin aluminum foils mounted on cardboard cards or aluminum frames. Foils of 2.2, 4.4, 6.0, 9.0, 14.0, 19.5, 34.0, and 39.0 mg/cm^2, are available. The thicknesses used in such an extrapolation are dependent largely upon the total range of the beta particles being measured. Thus with C^{14} particles (range = 25 mg/cm^2) it would be unwise to carry the curve much further than 10 mg/cm^2 while with RaE (range = 410 mg/cm^2) it should be possible to obtain a linear extrapolation out to 50-60 mg/cm^2.

The equation for such an exponential curve may be expressed as:

$$\frac{N_x}{N_o} = e^{-mx}$$

where N_x is the counting rate as measured, N_o is the extrapolated or true counting rate, m is the slope of the curve, and x is the thickness of the window and air. The slope may be obtained from the absorption curve and the N_o value calculated for any window of known and reasonably small thickness.

A series of values for "m" as measured for various isotopes is given in Table 2.

It will be noted that these coefficients do not necessarily correlate exactly with the particle energy. This is believed to be due to possible difference in the low energy end of the spectrum allowing variations in the fraction absorbed in a thin shield.

In using the values of the absorption coefficient it is convenient to define a factor, f_a, which is equal to $\frac{N_o}{N_x}$ and which when multiplied by the observed counting rate will give the extrapolated or No' value.

Thus,

$$\log_e \frac{No}{N_x} = mx$$

$$\log_e f_a = mx$$

Table 2
BETA RAY ABSORPTION COEFFICIENTS IN ALUMINUM

Isotope	Energy Mev		Shelf 1	Shelf 2	Shelf 3	Shelf 4	Shelf 5
C^{14}	0.15		0.304				
S^{35}	0.17		0.269				
Co^{60}	0.30	Total	0.0882	0.0787	0.0792	0.0843	
		Gamma Corrected	0.105	0.0903	0.104	0.0909	
*Ce^{144}	0.35			0.107	0.102		
Cs^{137}	0.5 & 0.8		0.0253	0.0269	0.0244		
I^{131}	0.6 & 0.25			0.0310	0.0326	0.0311	
Au^{198}	0.6 & 0.97		0.0142	0.0139	0.0147	0.0165	0.0167
RaE	1.17	Mounted on .001" Al	.0186	0.0226	0.0260	0.0283	
		Mounted on .004" S. Stl.	.0193	0.0177	0.0194	0.0196	0.0216
Y^{91}	1.7		0.00518	0.00923			
P^{32}	1.7			0.00700			0.00923
*Pr^{144}	3.1			0.00230	0.00235		
Ru^{106} Rh^{106}	.03 & 3.9		0.00497	0.00546	0.00652	0.00619	

*Calculated from Ce^{144} - Pr^{144} absorption curve.

1083744

The value fa is always greater than one and will vary with total absorber, x, between source and active volume of counter.

The accuracy with which the N_o value may be obtained using the coefficients in Table 2 depends greatly upon the energy of the emitter and the total absorber through which the extrapolation must be made. For energies of 0.6 Mev and higher the error introduced into the factor fa because of uncertainty in the value of the absorption coefficient is estimated to be $\pm 0.5\%$ for each mg/cm^2 of air-window absorber.

For lower energies large errors may be introduced in the f_a value because of the steepness of the absorption curves (high value of absorption coefficient) and because the absorber thickness through which extrapolation is made becomes an appreciable fraction of the total range. Effects of self-absorption become more prominent. An example of this accuracy achieved in the measurement of C^{14} by the Development Group is discussed in a later section.

1083745

C. Spread of Source

In preparing a source for measurement it is not always possible to place the activity in an area small enough so that it may be considered as a point source. In fact, for most routine measurements the sample is placed on 1-1/2" or 1" diameter plate and counted within 0.191" of a window 1-1/8" in diameter. The possibilities of loss in counting rate simply due to the change in solid angle from a point source in the center to the edge of the plate is immediately apparent. This factor becomes less important as the plate is moved away from the counter face.

A correction factor for a uniformly spread circular source may be obtained by measuring the counting rate of a point source at various points across the diameter of the tube, and integrating the rates after they have been weighted according to the area represented by an annular ring at that radius. This may most easily be accomplished by multiplying the individual counting rate by the radius at which it was measured and plotting a curve of counts per minute times radius versus the radius. The area under this curve is then proportional to the total counting rate expected from an extended source of radius equal to the abscissa considered on the curve. This area may then be compared to the area under the straight line representing the condition if no loss in counting rate were experienced.

Figure 8 represents the ratio of counting rates of point sources at various distances from the center of the tube to the counting rate on the axis. Also plotted are theoretical curves calculated from the geometrical conditions by the method presented in appendix I. The measured curves are the result of the average of three to six measurements on RaE. Figure 9 presents a plot of counting rate times the radius versus the radius at which the points were measured. The areas under the curves are measured with a planimeter out to the radius of interest and the ratios between the two areas found. In general, the two curves obtained on both sides of the center are symmetrical within the counting error of the individual points.

1083746

Although it was presumed that little if any difference would be noted with different energy particles except in the low ranges where a small difference in absorption thickness would be significant, curves were measured for C^{14}, I^{131}, RaE, and Ru^{106}- Rh^{106}. The results from these four sources expressed as fractions of the counting rates at the given radius that would be obtained for a point source of the same activity are given in Table 3.

Table 3
RATIO OF SPREAD SOURCE COUNTING RATE TO POINT SOURCE COUNTING RATE FOR EQUALLY ACTIVE SOURCES, fd.

RaE					
Shelf	0.50" Diam.	1.00" Diam	1.50" Diam	2.00" Diam	2.50" Diam.
1	0.95	0.84	0.59	0.39	0.25
2	0.96	0.87	0.75	0.62	0.36
3	0.97	0.94	0.86	0.76	0.69
4	0.99	0.95	0.91	0.86	0.69
5	0.99	0.97	0.94	0.91	0.86
I^{131}					
Shelf	0.50 Diam.	1.00 Diam.	1.50 Diam.	2.00 Diam.	2.50 Diam.
1	0.95	0.83	0.60	0.39	0.26
2	0.96	0.87	0.82	0.67	0.54
3	0.97	0.91	0.85	0.77	0.68
4	0.99	0.95	0.91	0.86	0.81
5	1.00	0.96	0.92	0.89	0.86
Ru^{106} - Rh^{106}					
Shelf	0.50 Diam	1.00 Diam	1.50 Diam.	2.00 Diam	2.50 Diam.
1	0.94	0.76	0.54	0.39	0.26
2	0.93	0.88	0.79	0.66	0.54
3	0.97	0.93	0.87	0.80	0.73
4	0.98	0.96	0.92	0.88	0.82
C^{14}					
Shelf	0.50 Diam	1.00 Diam	1.50 Diam	2.00 Diam	2.50 Diam.
1	0.95	0.79	0.51	0.32	0.22
2	0.93	0.84	0.68	0.53	0.41
3	0.99	0.90	0.79	0.68	0.52
4	0.99	0.93	0.86	0.77	0.68
5	0.99	0.94	0.90	0.83	0.75

1083747

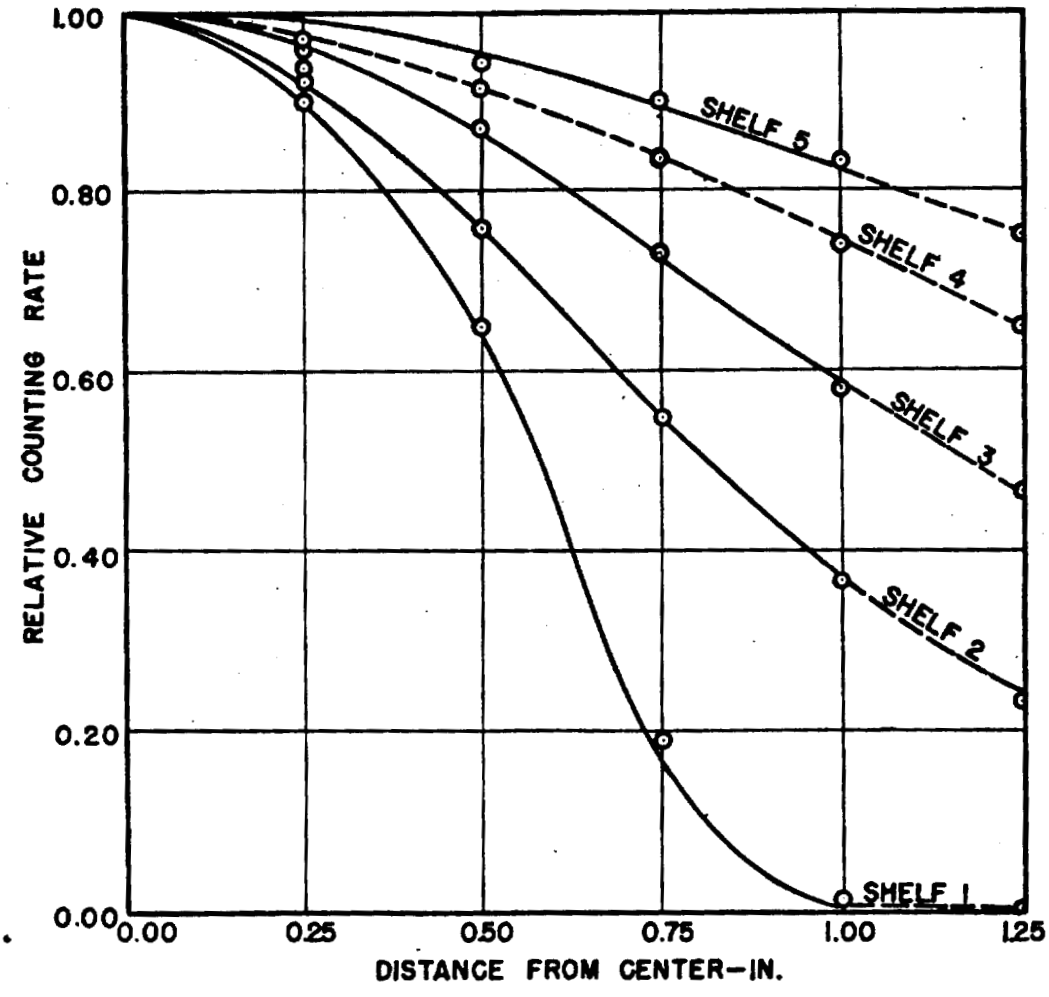

FIG. 8. VARIATION IN COUNTING RATE OF A POINT SOURCE WITH RADIAL DISPLACEMENT OF SOURCE FROM THE VERTICAL COUNTER AXIS. SOLID LINES ARE CALCULATED VALUES. PLOTTED POINTS ARE EXPERIMENTAL DATA.

1083748

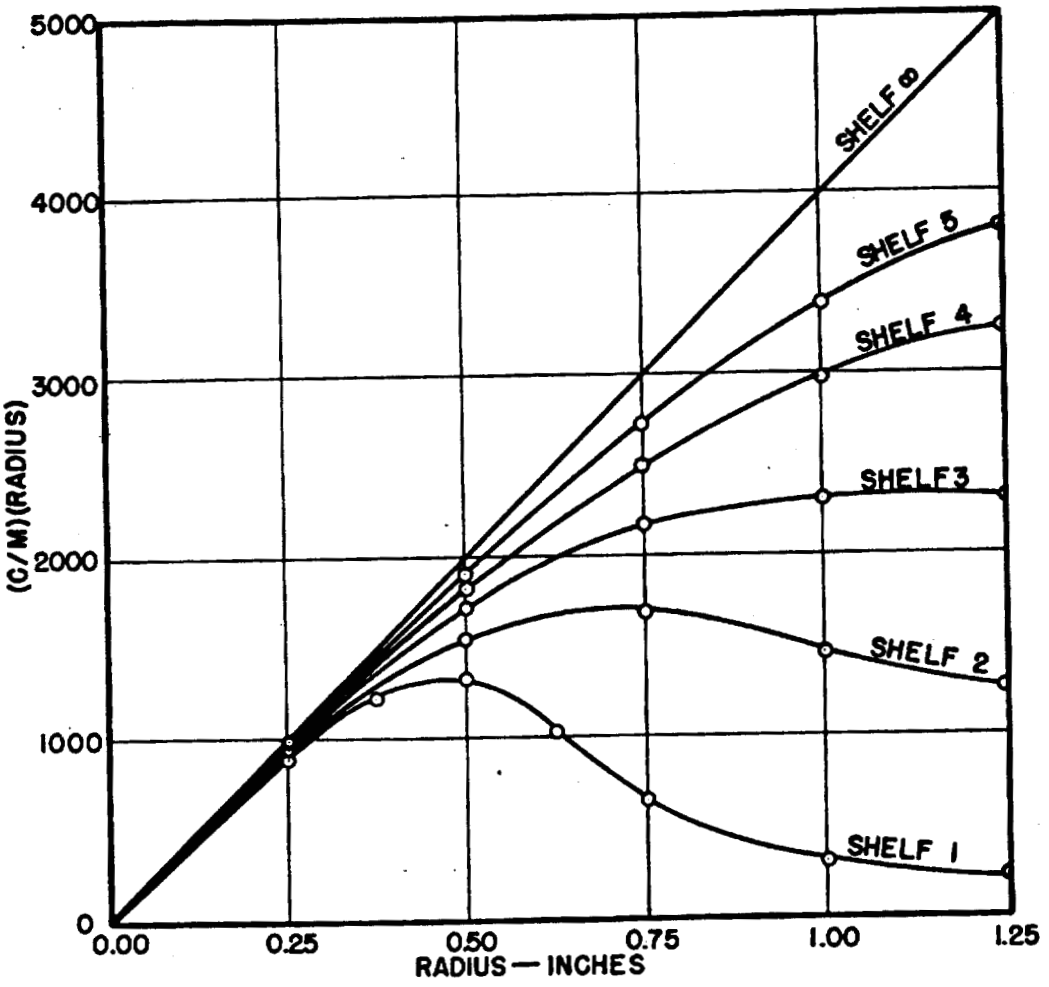

FIG. 9. VARIATION IN WEIGHTED COUNTING RATES WITH RADII OF ANNULAR SOURCES (RADIUM E)

Included also are data for various shelves to illustrate the expected decrease in importance of this factor when extended sources are placed at greater distances from the counter window. The data appears to indicate that for very soft beta emitters such as C^{14}, the factor is significantly different than when emitters of higher energy such as the 1.17 Mev beta particles from Radium E are measured. In general, the factors as measured for the Radium E source should be applicable to moderate energy materials.

D. Geometry

The geometry of a counter is often loosely referred to as the ratio of the counting rate to the disintegration rate of the source, or to the number of beta particles emitted per minute from the source. This concept is acceptable when samples of the same type and size, mounted in the same manner are being counted. In this case an overall correction factor including scatter, absorption and actual geometry may be lumped into a single correction factor. When different isotopes mounted in various manners and counted on different units are being measured, each of these correction factors must be taken into account separately if the results are to be compared. In this work the geometry has been considered as the ratio of the solid angle subtended by the aperture of the sensitive volume of the tube to the 4π solid angle, with the source at the origin. This has been obtained by correcting the counting rate of a source of known disintegration rate for all known factors such as scatter, absorption, etc., in the manner already described and recording the ratio of the corrected counting rate to the disintegration rate of the source as the solid angle correction, or energy-independent geometry.

The exact expression for the ratio of the solid angle formed by the intersection of the counter window with a sphere with its center at the source and on the axis of the counter, and radius equal to the distance from the point source to the periphery of the window, to the total solid angle about the point is given by:

1083750

$$G = \frac{2\pi R(R-h)}{4\pi R^2} \qquad (1)$$

in which,

R = Radius of the sphere (distance from point source to the periphery of the counter window.)

h = Distance from the source to the window.

which reduces to,

$$G = \frac{R-h}{2R} \qquad (2)$$

or in terms of the radius of the window, b,

$$G = \frac{1}{2}\left(1 - \frac{h}{\sqrt{h^2 + b^2}}\right) \qquad (3)$$

The value of G calculated using this equation is generally higher than the experimentally determined value when it is assumed the distance h is measured from the source to the plane of the counter window. Other investigators (13) have postulated a possible dead space extending three or four millimeters up into the tube away from the window and have obtained agreement between their results and the calculated value by adjusting the distance, h. Since no values are available upon the actual depth of dead space beyond the window, no attempts have been made as yet to correlate the calculated geometry with the observed geometry.

Geometry of the sets in use has been obtained through measurement of sources from RaD, RaE, RaF chain in two manners: (1) a source prepared and calibrated by the Bureau of Standards, consisting of a palladium coated silver disc upon which RaD has been electroplated, has been used as a primary standard; (2) sources prepared in this laboratory by evaporating small amounts of RaD, E, F solution on a very small area in the center of an aluminum disc are counted daily as routine control sources. These control sources have been calibrated by counting on the standard 52% geometry alpha counter and correcting the counting rate for coincidence losses. It was also found that during evaporation of the liquid a small amount of the daughter, RaF(Po), whose alpha particles are counted in the alpha counter, was lost, thereby destroying the equilibrium between RaD, E, F. The sources have exhibited an alpha build-up, and from the monthly alpha counts made it has been possible to calculate the equilibrium RaF disintegration rate which will eventually

be reached. The sources are covered with 3.1 mg/cm^2 of cellophane to shield out the alpha particles from RaF, and the very soft RaD beta particles (0.025 Mev). The beta counting rate of these sources is corrected for absorption in the mica window as outlined in Section B, and for backscatter from the aluminum mount by the factor 1.29 given in Section IV-A. The resulting geometries for several of the sets are given in Table 4. The Bureau of Standards source was corrected for backscatter by the factor of 1.58 given for silver in Section A, and for absorption in the air and window. In addition a correction factor of 5.3% was found necessary because of the spread of the activity over a one-half inch diameter on these sources. This factor was determined by the method given in Section C, making accurate determinations with points measured each 1/16 of an inch across the diameter of the counter. The values of the geometry obtained with the Bureau of Standard sources are also given in Table 4 for comparison.

1083752

Table 4

POINT SOURCE GEOMETRY OF MICA WINDOW GM TUBES, APRIL 1950

Set No. -Tube No.	Window mg/cm^2	Geometry from Count on Control Sources, RaDEF on Aluminum	Geometry from Count on U.S.B.S. RaDEF Source				
			1st	2nd	3rd	4th	5th
1-158	4.5	0.241	0.233	0.0738	0.0333	0.0185	0.0122
2-164	4.6	0.239	0.233	0.0739	0.0330	0.0180	0.0120
3-139	2.9	0.236	0.230	0.0730	0.0328	0.0186	0.0117
4-119	2.9	0.248	0.239	0.0757	0.0333	0.0191	0.0117
5-136	3.4	0.233	0.231	0.0735	0.0327	0.0182	0.0117
6-185	3.0	0.220	0.226	0.072	0.0320	0.0180	0.0116
7-128	4.1		0.234	0.0739	0.0330	0.0182	0.0117
8-112	4.6	0.239	0.236	-	-	-	-
9-103	3.2	0.241	0.233	0.0730	0.0330	0.0169	0.0115
10-168	4.5	0.240	0.232	0.0728	0.0326	0.0180	0.0117
11-155	4.3	0.220	0.219	0.0697	0.0309	0.0174	0.0115
12-161	3.4	0.212	0.218	0.0699	0.0315	0.0178	-
13-5A-60 (Tracerlab Tube)	2.4	0.215	0.216	0.0733	0.0331	0.0185	0.0118
14-184	3.7	0.250	0.240	0.0740	0.034	0.0190	0.0120
15-148	3.5	-	0.223	0.0708	0.0325	0.0183	0.0120

1083153

The reasonably good agreement between these two sets of data indicate that at least the backscatter correction which we apply cannot be in error by more than a few percent. It also serves to substantiate the value of 52% used for the geometry of the Standard Alpha counters on which the control sources were calibrated.

E. Self-Absorption

When a counting plate is prepared from an analytical sample, a significant amount of residue is usually obtained unless the sample is so active that only a small amount may be used. The amount of this residue may seriously affect the results due to self-absorption of the particles and to some extent to scatter of particles by the residue into the counter. The mechanism of beta scatter and beta absorption is extremely complicated due to the wide spectrum of the energy of the particles and this phenomenon is practically impossible to calculate from theoretical data. In general, correction factors are obtained by preparing plates with known amounts of precipitated carrier and known amounts of activity and obtaining empirical self-absorption curves. Other investigators have published such curves for numerous materials, (5,6, 12) but in general it is felt that such correction factors should be obtained with the particular techniques and equipment being used by the individual performing the work. Self-absorption curves for several materials are plotted in Figures 10 and 11. These curves are plotted as fraction of the activity measured versus the thickness of precipitate spread on a one and one-half inch stainless steel plate and counted on the first shelf. The curves for S^{35}, C^{14}, Fe^{59}, and Ca^{55} are of particular interest and importance because of the extremely large self-absorption encountered with these soft beta emitters. It is of interest to note at this point that the C^{14} curves obtained in this laboratory agree very closely with those obtained by Dr. Yankwich at the University of California.(12) One interesting phenomenon with a soft beta emitter such as C^{14} is the relative independence of the counting rate on amount of material once a certain critical thickness is reached. Thus, with more than 25 to 30 mg/cm^2 of barium

1083754

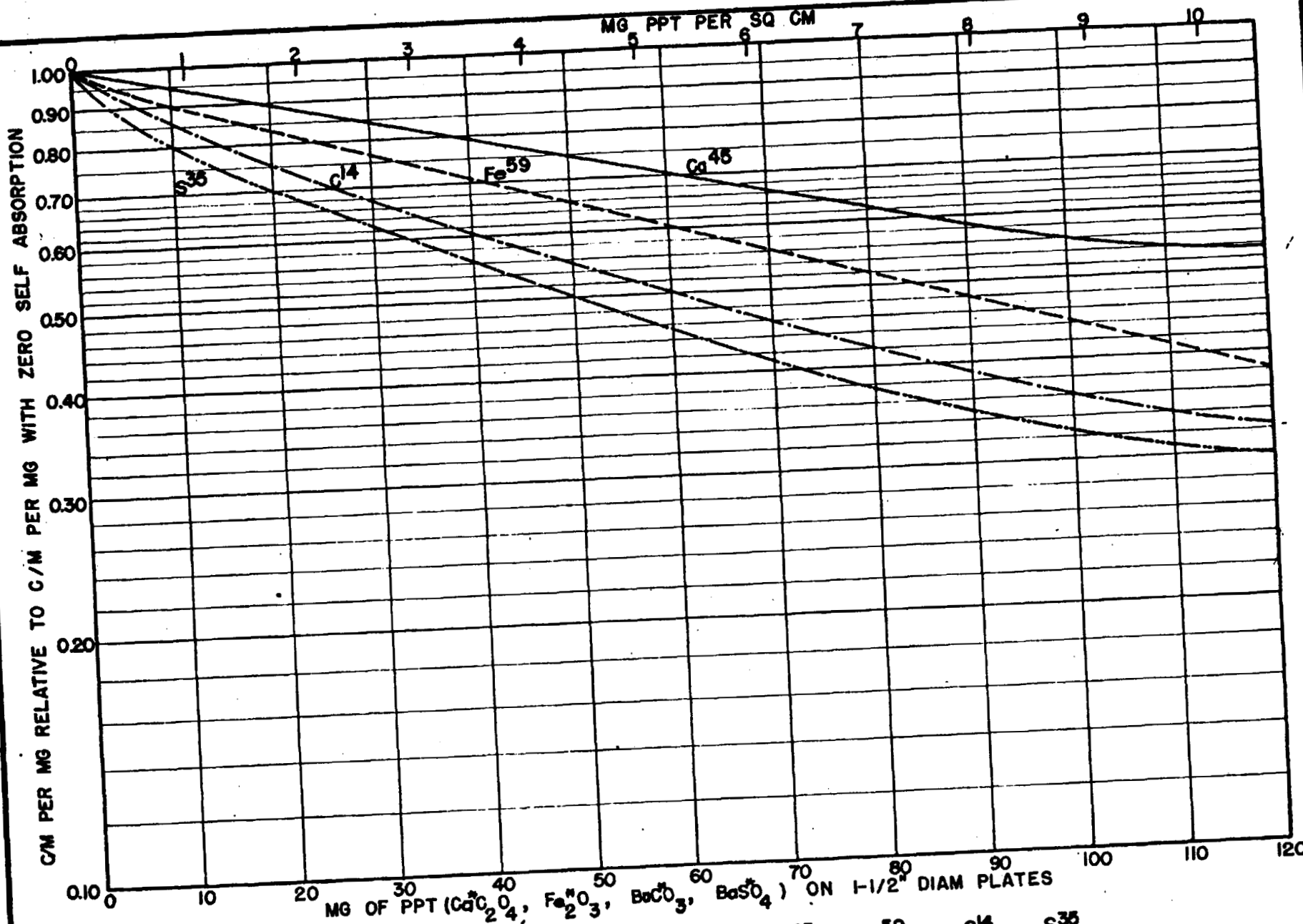

FIG. 10 SELF ABSORPTION CURVES: $_{20}Ca^{45}$, $_{26}Fe^{59}$, $_{6}C^{14}$, $_{16}S^{35}$

1083155

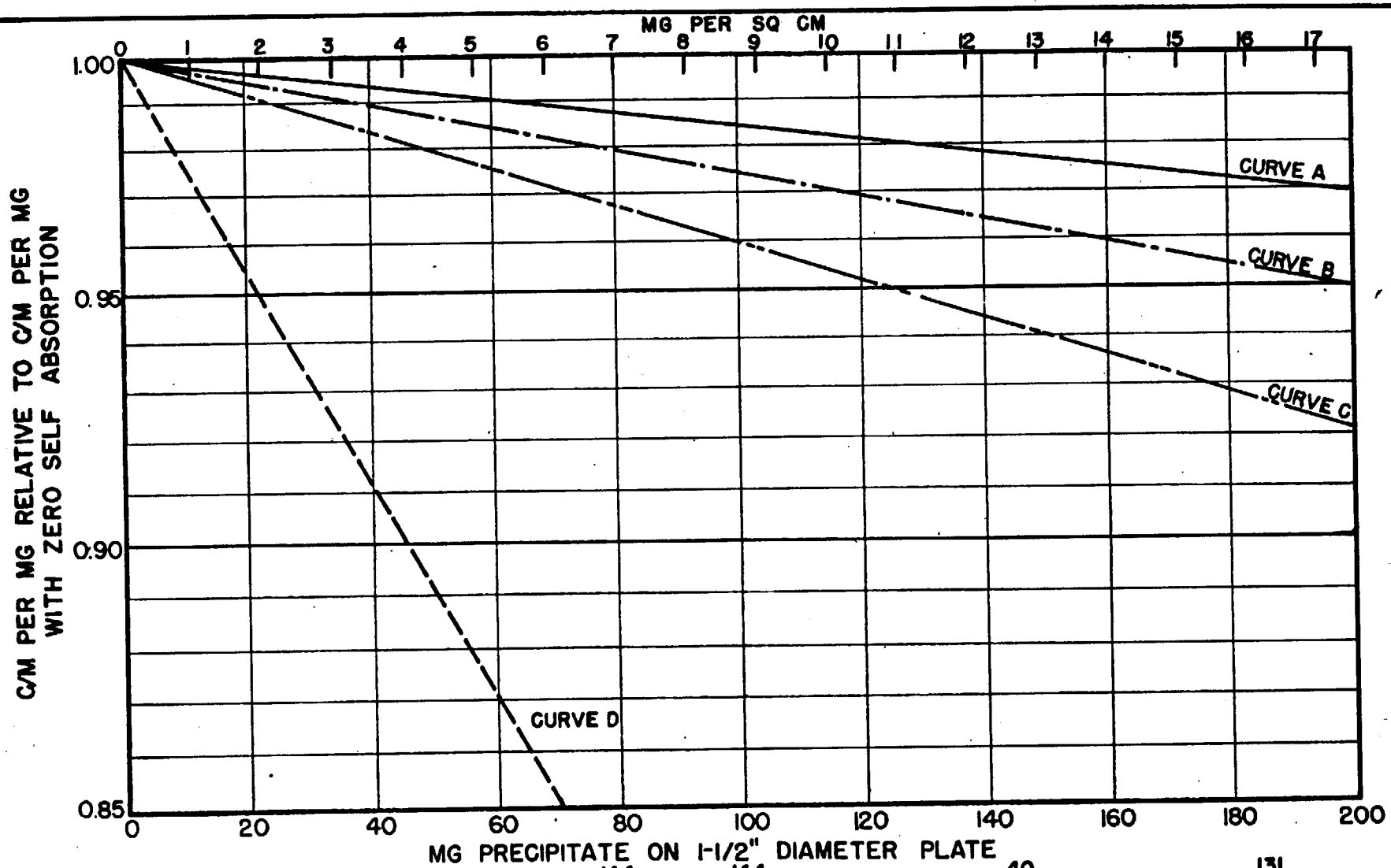

CURVE A: $Sr^{90}C_2O_4 - Y^{90}C_2O_4$; CURVE B: $Ce^{144}(OH)_3 - Pr^{144}(OH)_3$; CURVE C: $K^{40}Cl$; CURVE D: AgI^{131}

FIG. 11 SELF ABSORPTION CURVES FOR HIGHER ENERGY EMITTERS

1083156

carbonate on the plate in the measurement of C^{14}, the counting rate is proportional to the specific activity or curies per gram of the material rather than on the total amount on the plate. The use of mica window counters for the measurement of C^{14}, S^{35}, etc. is perfectly acceptable when large amounts of activity are present. It is not as sensitive as some of the other methods outlined in the literature (13, 14, 15), but can be used acceptably if counting rates of 10 to 20 counts per minute above background on a sample may be obtained. In any case the self-absorption correction factor plus the factor for absorption in the window and air and for backscatter should be determined in order to obtain absolute values.

An interesting consequence of self-absorption was obtained when a request to calibrate a small uranium chip for use as a counting standard was obtained. The small chip of uranium metal weighing approximately 100 mg was counted on the first and second shelves and the results calculated to apparent disintegrations per minute using the geometries obtained by the Radium D standards for these shelves. The measurement on the first shelf indicated 4980 beta particles per minute, while the measurement on the second shelf indicated 6530 beta particles per minute. An experiment in which inactive cerium nitrate was added to radio-ruthenium on a one and one-half inch stainless steel plate indicated that the increase in apparent disintegration rate on the second shelf was actually real and was probably due to a self-absorption factor.

A qualitative explanation of the effect, suggested by C. C. Gammertsfelder, involved the differences in path length in the material for beta particles emerging from a small rectangular chip at various angles. Thus the particles arriving at the counter on the first shelf include those which come out at a greater angle to the normal than those on the second shelf. The effective path length in the uranium is thus longer resulting in an effective decrease in the measured activity. An attempt was made to obtain a semi-quantitative measure of the effect by calculating the absorption from a RaE spectrum and data on the penetration of particles.

1083757

(See appendix II). A correction factor of 69% for absorption in the uranium on the first shelf, and 94% on the second shelf was obtained. When these values were applied to the measurement, values of 7200 and 6960 beta particles per minute were obtained for the first and second shelves respectively.

The above explanation was given additional weight by the results of an experiment wherein a chip of uranium 0.173 mm thick was mounted on a support which could be rotated about a horizontal axis. Directly over the center of the source a slit was placed to allow only a narrow beam of rays directly from the center of the uranium chip to enter the counter window. This holder was placed on the second shelf and the chip rotated in steps of 10 degrees up to 70 degrees and the counting rate determined for each angle. Each value obtained in this manner was multiplied by a constant which made the initial point fall directly on the value for fraction transmitted at 0° as developed above. As the angle increased the counting rate fell off and at a rate in fair agreement with the calculated values. Both the calculated curve and the measured curve are given in Figure 12.

F. Miscellaneous

For most of the routine work no correction is made for the contribution to the counting rate caused by gamma radiation, because of the low efficiency of the particular type of counters used. This in general means that the rate for the routine samples will be higher than the true rate and will therefore serve as a safety factor in health measurements. For accurate work however, it is necessary to obtain a value for the beta radiation only. This is generally accomplished by the use of an aluminum absorber of such thickness as to allow complete absorption of the beta particles but minimum absorption of the gamma photons. Thus when dealing with a beta particle of 1.5 Mev sufficient aluminum would be inserted between the sample and the source to cut out the beta particles and possibly leave about 5-10% excess aluminum as a safeguard. These absorbers are inserted as close as possible to the counter so as to minimize scatter effects. The small contribution of secondary electrons from the face of the shield is ignored

1083758

since it is felt that this amount of radiation would involve a very small error compared to the magnitude of errors in the other factors such as absorption in the window, backscatter, etc.

No specific determination for the coincidence losses has been made although this would be possible by the same technique described under the alpha counting. In general, a value of 0.2% loss per thousand as quoted in the literature for this type of counting equipment has been used.

The greatest single factor in causing errors and non-reproducible results in our counting has been the spread of the activity on the counting plate. The plates used have sharp corners at the edges and the material being evaporated tends to agglomerate in these corners giving a ring of activity at the outer circumference of the plate. Since this ring of activity is at a considerable distance from the center of the tube the geometry for counting is low and a low value compared to the correction factor obtained in the section on spread of the source is obtained.

Radioautographs of the plates prepared with small amounts of carrier are given in Figure 13. Since this is a more or less random effect and dependent upon the techniques used, the temperature at which the evaporation is carried out, the amount of carrier present, etc., the values for a given series of plates will fluctuate over a much wider range than would be expected from sheer counting chance. It has been difficult to eliminate this in the past because of the desirability of having plates on which several milliliters of liquid may be evaporated. Experimental plates smaller in diameter with the corners curved so as to eliminate sharp break at the circumference of the plate are now being used. It is believed that this will produce a large improvement since it will tend to eliminate the agglomeration at the corner and will make a smaller area for the counter tube to view.

1083759

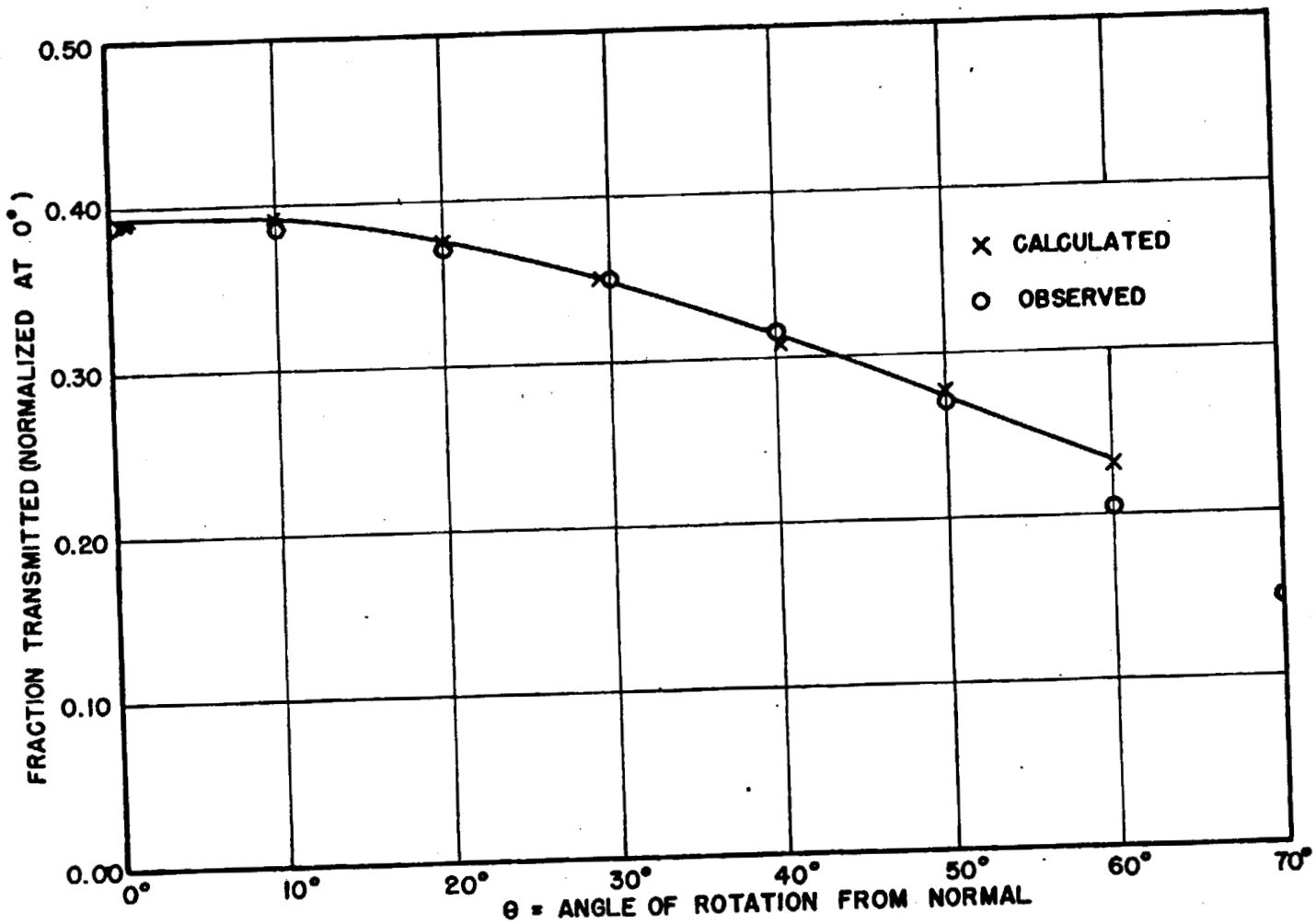

FIG. 12. ANISOTROPIC DISTRIBUTION OF BETA PARTICLES EMITTED FROM A URANIUM CHIP.

0083160

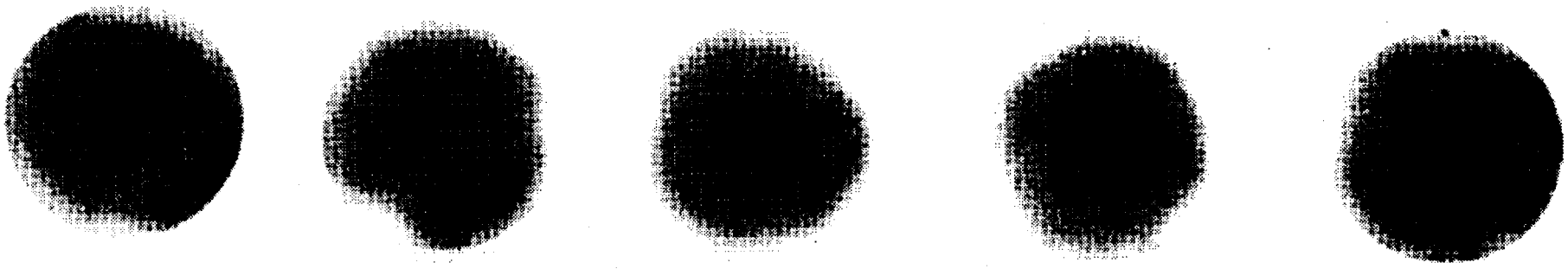

PLATES CONTAINING CARRIER (20 MG OF CERIUM AS THE HYDROXIDE)

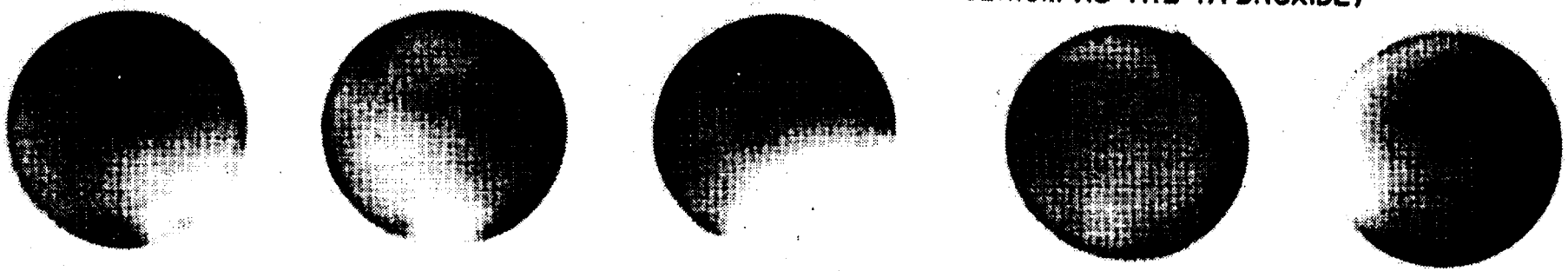

PLATES WITHOUT CARRIER

FIGURE 13

RADIOAUTOGRAPHS OF 1 1/2" PLATES CONTAINING $Ce^{144}-Pr^{144}$ ACTIVITY EVAPORATED WITH AND WITHOUT CARRIER.

DARKENED AREAS CORRESPOND TO HIGHER ACTIVITY. LESS UNIFORM SPREADING AND CONCENTRATION AT THE RIM EXHIBITED BY PLATES DRIED WITHOUT CARRIER.

1083101

V. Discussion

The estimated accuracy of the calibrations employed are such that the final evaluation for a point source with no self-absorption should be within ±5% of the true value for moderate energy emitters. The error may be slightly greater for low energies (0.15 - 0.4 mev.) The most serious errors are believed to be due to non-uniform spreading on the sample plate. Since the solution concentrates around the edges, the bulk of the material is counted at a low geometry. The use of one inch plates for beta counting has greatly assisted in more uniform results.

These calibrations are used to estimate activities in samples by calibrating a solution of the activity to be measured and obtaining the overall yield of the chemical and counting process by analyzing aliquots of this calibrated solution along with the samples. Thus an overall value of the chemical and counting yields may be obtained and expressed as c/m per microcurie in the sample. (Microcurie is defined for this work as that amount of material that emits 3.7×10^4 beta particles per second) Generally such solutions may be active enough so that the aliquot used can be placed on a very small area thus giving essentially a point source with no self-absorption.

Several checks on the counting have been made by comparison with other methods and other laboratories. A comparison of I-131 sources carried out for the purpose of studying the chemistry of iodine gave the results listed in Table 5[14].

Table 5
I^{131} MEASUREMENTS BY THREE METHODS

Source #	Value by Beta Counting	Value by Coincidence Counting	Value by Vacuum Low Geometry Counter
	d/m	d/m	d/m
P	$5.60 \times 10^6 \pm 1.6\%$*	$6.29 \times 10^6 \pm 5.6\%$*	$6.08 \times 10^6 \pm 1.6\%$*
Q	$11.44 \times 10^6 \pm 1.0\%$	$11.11 \times 10^6 \pm 4.6\%$	$10.65 \times 10^6 \pm 1.5\%$

* Error indicates counting error only on 90% confidence level.

1083762

The coincidence results were corrected by estimated values for the difference between the beta ray spectrum listed by Kern, Mitchell, and Zaffarano[15] and a simple cascade scheme. The vacuum low geometry device is an instrument constructed at this laboratory to allow the measurement of a well collimated beam of beta particles with a mica window tube. More details of both methods will be issued in a later report.

One sample of C^{14} was obtained from Dr. Hennig at Argonne National Laboratory. This sample was calibrated very carefully for use in a measurement of the half-life of C^{14}. His value was $(1.15 \pm 0.014) \times 10^5$ d/m;[16] the value obtained in this laboratory using mica window counters was $(1.22 \pm 0.029) \times 10^5$ d/m, a 6.1% difference.

These cross-checks would seem to indicate that the values quoted in this report are reasonably consistent with the true values. Further work is planned to eliminate present small errors due to instrument peculiarities and to further refine the correction values presented in this report.

1083763

APPENDIX I

I. Calculation of Geometry for Off-Center Source.

The problem consists of measuring the solid angle subtended by the counter face and a point. This may be accomplished by calculating the area subtended on a sphere of radius OA (See Figure 14) by the Figure OAB where AB is a projection of the counter window on the XOZ plane with the source located at the origin, O.

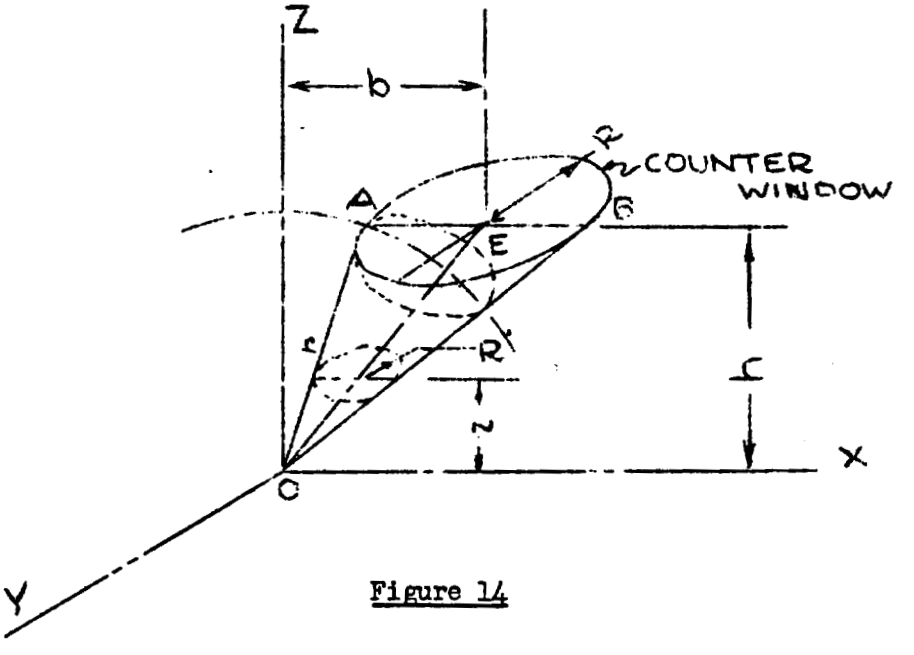

Figure 14

The equation of the solid Figure ABO may be calculated by considering that planes parallel to the XOY plane will cut out circles of different radii. The radius of the circle is given by:

$$(1) \quad \frac{R'}{z} = \frac{R}{h}$$

Where h is the perpendicular height of the counter face above the source, z is the height of the general circle of radius R', and R is the radius of the counter.

$$(1a) \quad R' = \frac{R}{h} \quad z$$

1083764

The position of the center is given by the equation of the line EO.

$$(2) \quad z = \frac{h}{b} x$$

There b is the displacement of the source (at origin) from the center of the counter window.

Thus the equation of the surface is:

$$(3) \quad (x - \frac{b}{h} z)^2 + y^2 = \frac{R^2}{h^2} z^2$$

If the length of the line AO is represented by r, the equation of a sphere with origin at the center through the point A is:

$$(4) \quad x^2 + y^2 + z^2 = r^2$$

Eliminating y between equations (3) and (4) to obtain the trace in the XOZ plane:

$$(5) \quad z^2(\frac{b^2}{h^2} - \frac{R^2}{h^2} - 1) - \frac{2b}{h} zx + y^2 = 0$$

The area of intersection is then given by:

$$(6) \quad A = \int_a^{a'} \int_b^{b'} \left[1 + \left(\frac{\partial y}{\partial z}\right)^2 + \left(\frac{\partial y}{\partial x}\right)^2\right]^{\frac{1}{2}} dzdx$$

Where the limits a and b are obtained from the trace in the XOZ plane.

Solving equation (5) for z:

$$(7) \quad z = \frac{bx \pm \sqrt{b^2 x^2 - K}}{L}$$

Where $K = r^2(b^2 - R^2 - h^2)$

$$L = \frac{K}{r^2 h}$$

This expression will give the lower limits for z on the integration when the negative sign is used. The upper limit is given by the equation of the circle projected on the XOZ plane by the sphere.

The limits for x are obtained by simultaneous solution of the equation of the trace of the sphere in the XOZ plane and the equation of the line from the origin to the edge of the counter, OB.

1083765

Thus the area of intersection is given by:

$$(8)\quad \text{Area} = \int_{b-r}^{\sqrt{1+\left(\frac{h}{b+r}\right)^2}\,r} \int_{\frac{bx \pm \sqrt{b^2x^2 - K}}{L}}^{\sqrt{r^2 - x^2}} \frac{r}{\sqrt{r^2 - x^2 - z^2}}\, dz\,dx$$

After the first integration and substitution of limits

$$(9)\quad \text{Area} = r \int_{b-r}^{\sqrt{1+\left(\frac{h}{b+r}\right)^2}\,r} \left[\frac{\pi}{2} - \arcsin \frac{bx \pm \sqrt{b^2x^2 - K}}{B\sqrt{r^2 - x^2}}\right] dx$$

Since this expression is difficult to integrate, it was decided to solve for the points of interest by graphical methods. The integration is summed in Table 6.

1083766

Table 6

SOLUTION OF EQUATION FOR COUNTER GEOMETRY

h	b	Area of Intersection	Total Area of sphere	Calculated Geometry	Calculated Geometry for Pt. Source in Center	Ratio
0.1911"	0.25	0.5354	1.686	0.3176	0.339	0.937
	0.50	0.1100	0.5076	0.2168		0.639
	0.75	0.0483	0.9003	0.0536		0.158
1	1.00	0.0367	2.864	0.0128		0.038
0.816"	0.25	0.7814	9.595	0.0814	0.0883	0.922
	0.50	0.5632	8.417	0.0669		0.758
	0.75	0.4250	8.809	0.0482		0.546
	1.00	0.3562	10.77	0.0331		0.375
1.441"	0.25	0.9190	27.32	0.0336	0.0343	0.980
	0.50	0.7800	26.14	0.0298		0.869
	0.75	0.6612	26.54	0.0249		0.726
	1.00	0.5762	28.50	0.0202		0.589
2.691	0.25	0.9422	92.23	0.0102	0.0106	0.965
	0.50	0.9270	91.05	0.01018		0.962
	0.75	0.8556	91.44	0.00936		0.885
	1.00	0.8234	93.40	0.00981		0.833

1083767

APPENDIX II
CALCULATION OF THE EFFECT OF ANISOTROPIC DISTRIBUTION OF BETA PARTICLES FROM A URANIUM CHIP ON THE APPARENT DISINTEGRATION RATE

A graphical analytical method can be used to reconcile the apparent discrepancy between the beta particle emission rate from a uranium chip determined by counting the chip under two different geometries. The experimental observation to be explained is that the emission rate as calculated from second shelf counting rate is markedly higher than that calculated from counting the same source on the first shelf, assuming that self absorption losses are equal at both geometries.

Assume a chip of small area and a thickness of 0.3 mm. Calculate the equivalent path lengths in air of the paths of particles from points within the chip to the surface of the chip moving at angles θ_1, θ_2, θ_3, etc., from the normal. This is done for points at various distances, "t", below the surface, See Fig. 15.

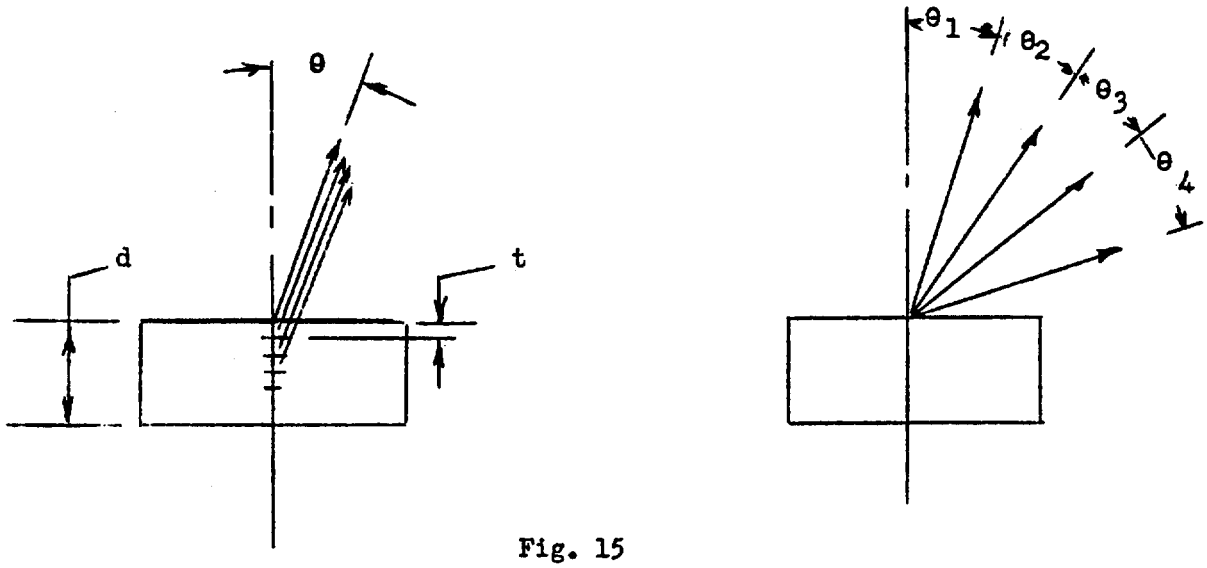

Fig. 15

Using this data for the equivalent air distance traversed by particles in escaping from the uranium chip, a corresponding energy can be assigned to each path length which will be the beta energy required to just traverse this distance in uranium. Assuming that the energy distribution curve for uranium betas is similar to that of RaE, the fraction of betas having an energy greater than that required to just get through the chip along an angle θ, and from a point "t" mm below the surface can be calculated. A table or graph can then be prepared

1083768

relating the fraction of beta particles transmitted at various angles for a series of assumed depths below the surface. Table 7 presents data obtained to a depth of 0.12 mm.

A plot is then made of fraction transmitted versus depth below the surface for the various assumed angles. See Fig. 16.

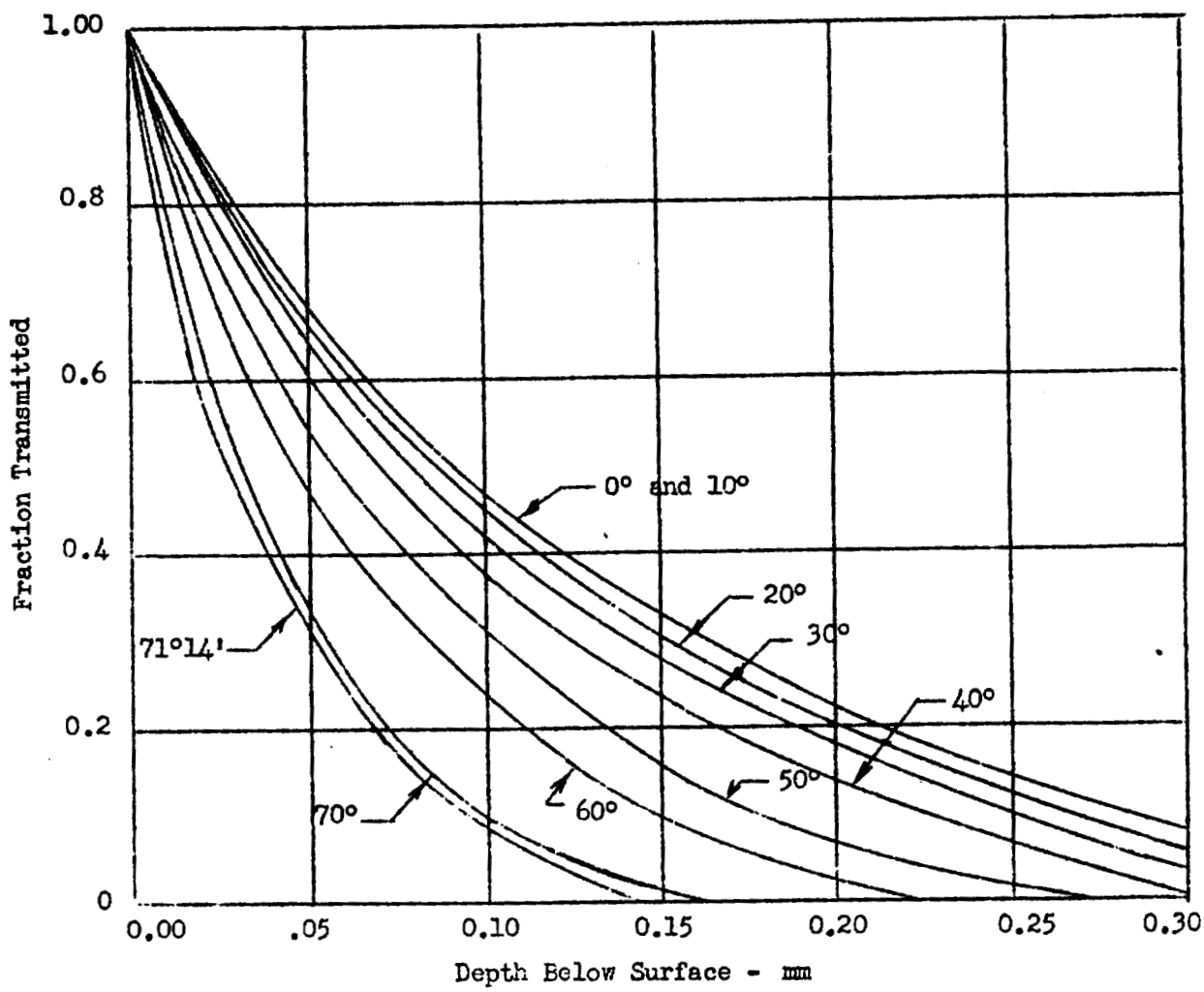

Fig. 16 Calculated Fraction of Hard Betas Transmitted Thru Uranium Metal

1083769

1083170

Table 7

θ Angle of Ray with Vertical)	Equivalent path length in cm. of air of beta particles traversing uranium from a point "t" mm below the surface and moving at an angle θ from the vertical; beta energy corresponding to this range, E; and fraction of betas escaping, N, along this path.																				
	t=0.01mm			t=0.02mm			t=0.04mm			t=0.06mm			t = 0.08mm			t = 0.10mm			t = 0.12mm		
	cm. air	E	N	cm. air	E	N	cm. air	E	N	cm. air	E	N	cm. air	E	N	cm. air	E	N	cm. air	E	N
0	14.5	.14	.90	29.	.18	.85	58.0	.32	.72	87.0	.42	.62	116	.50	.55	116	0.58	.46	174	.66	.39
10	14.7	.14	.90	29.4	.18	.85	58.8	.32	.72	88.2	.43	.62	118	.50	.55	147	0.58	.46	177	.67	.39
20	15.4	.14	.90	30.8	.20	.84	61.6	.34	.71	92.4	.44	.61	124	.53	.53	154	0.61	144	186	.68	.36
30	16.7	.14	190	33.4	.22	.82	66.8	.35	.69	100.	.46	.59	133	.54	.50	.67	0.64	.41	200	.72	.34
34° 25'	17.5	.15	.90	35.0	.23	.82	70.0	.36	.67	105	.47	-	140	.58	-	175	0.66	-	-	-	-
40°	18.9	.16	.89	37.8	.25	.79	75.6	.38	.65	113	.48	.55	151	.60	.46	189	0.69	.36	227	.78	.30
45°	20.5	.17	.89	41.0	.26	.76	82.0	.40	.62	123	.53	-	163	.62	-	205	0.73	-	-	-	-
50°	22.6	.18	.88	45.2	.28	.75	90.4	.44	.60	135	.56	.49	181	.67	.38	226	0.78	.30	271	.90	.24
60°	29.0	.23	.85	58.0	.32	.72	116.	.52	.53	174	.66	.39	232	.79	.30	290	0.93	-	348	1.08	.17
65°	34.3	.26	.77	68.6	.36	.66	137	.57	.47	206	.74	-	274	.90	-	343	1.07	.22	-	-	-
70°	42.4	.27	o.77	84.8	.41	.60	170	.64	.41	254	.85	.27	339	1.06	.17	424	1.27	.10	508	1.47	0.08
71°14'	45	.27	0.75	90.0	043	.57	180	.67	.38	27	.89	.24	360	1.11	.14	450	1.33	.08	540	1.54	0.06

The average fraction transmitted along a given angle is determined by measuring the area under the curve for the given angle, and dividing by the maximum abscissa or intercept. The actual values found are shown schematically in Fig. 17.

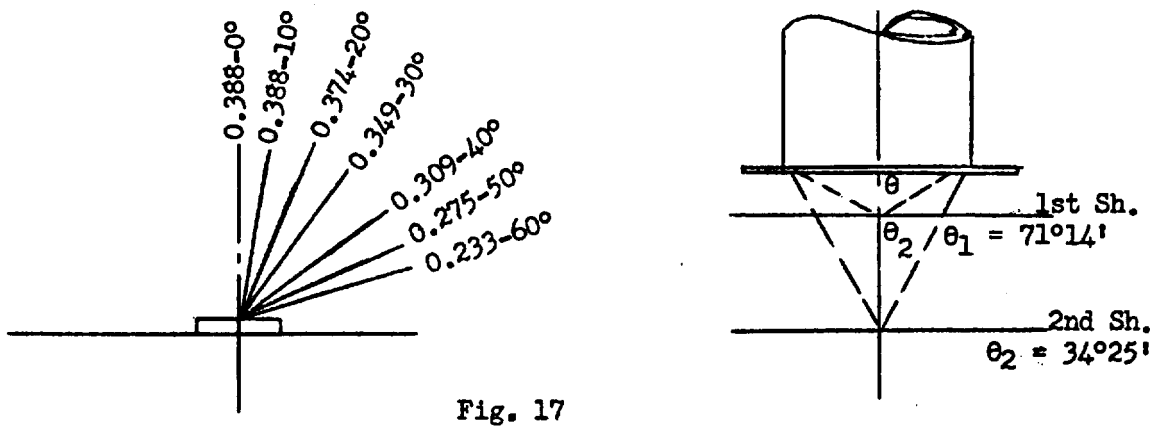

Fig. 17

The average fraction transmitted is weighted according to the area of the window which will "see" this fraction by multiplying each such fraction by the radius at which the ray enters the window. This value is plotted against the radius.

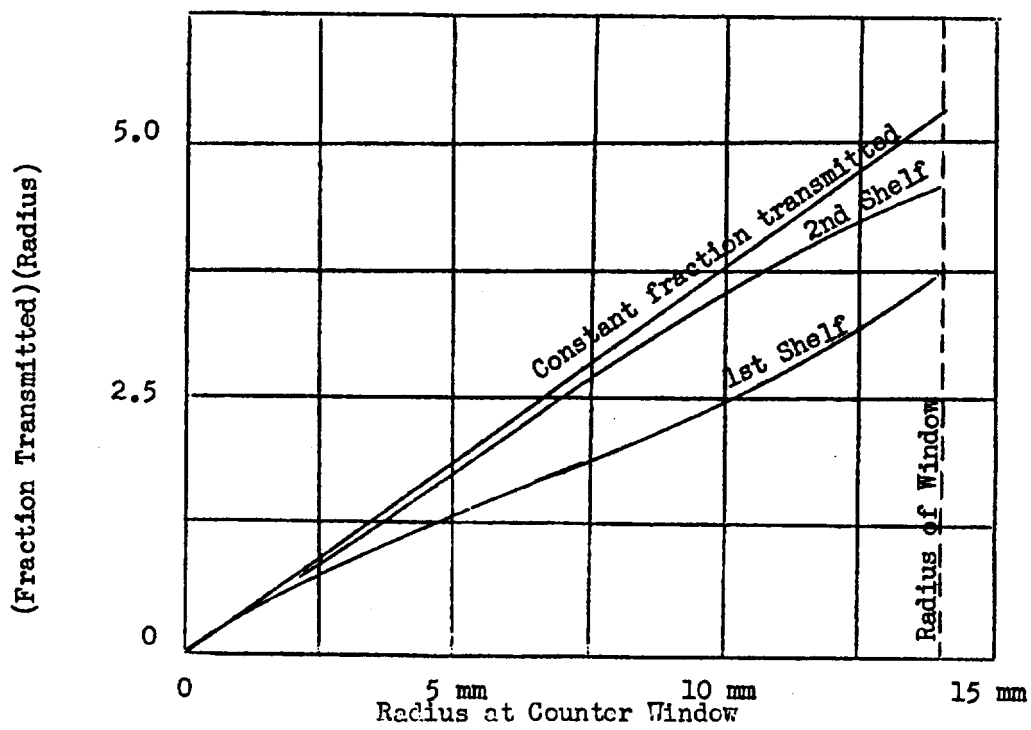

Fig. 18 Weighted Variation of Fraction Transmitted

1083771

If the beta radiation were isotropic, this plot should give a straight line passing through the origin with a slope determined by the fraction transmitted along the normal (0°) line. Since greater and greater losses are experienced with more obtuse path angles, the actual curve falls below the isotropic curve. The ratio of the area under the actual curve to that under the straight line is a measure of the relative fraction of beta particles arriving at the window.

As can be seen, for the second shelf this departure is much less than for the first shelf, since when the source is counted on the first shelf, a large fraction of the betas are lost in traveling through the longer paths at obtuse angles. The actual departure for the sample assumed by this development is 6% on the second shelf, and 31% on the second.

In effect, to normalize, or put both counts on a comparable basis, the count of a small thick chip of uranium on the second shelf should be divided by 0.94 and the count on the first shelf by 0.69. In the case examined these corrections brought the emission rate as calculated from first and second shelf counts into fair agreement.

It is obvious that this analysis can give but a roughly quantitative measure of the effect since several qualifying assumptions have been required, such as the shape of the beta spectrum for uranium. However it does confirm the concept that the geometry may play an important part in the self absorption correction factor for thick samples, and that the counting and mounting arrangement used when a self absorption curve is taken must be followed exactly if the correction factor is to be valid.

1083772

APPENDIX III
APPLICATION OF BETA COUNTER CALIBRATION DATA TO CALCULATION OF DISINTEGRATION RATES

The correction factors presented in the text are applied to the observed counting rate in the following manner.

$$d/m = \frac{(c/m)(fa)}{(G)(f_d)(f_{b.s.})(f_{s.a})}$$

In which,

d/m = disintegrations per minute

c/m = observed counting rate

fa = air-window absorption factor as defined in text.

G = point source geometry

f_d = sample diameter factor

$f_{b.s.}$ = backscatter factor

$f_{s.a.}$ = self absorption factor read from graph relating relative counting rate to weight of residue on plate. Used primarily for soft beta emitters.

In evaluating an analytical procedure for low level beta activity the following procedure is used. A solution is prepared containing a tracer quantity of the isotope for which analysis is to be made. This solution is standardized by preparing aliquots for counting by delivering 50λ or 100λ to the center of a plate of the type to be used in the analysis. The aliquot is allowed to dry essentially as a point source with no self absorption. From the counting rate and using the factors as described the disintegration rate of the "spike" can be calculated without the complication of non uniform spreading since the sample diameter correction becomes 1.00. The same aliquot is then used to "spike" blank samples, and the chemical extraction and precipitations performed exactly as with the unknown samples. The ratio of the c/m to the d/m of the aliquot of the spike is then used as an overall yield factor to arrive at the disintegration rate of the unknown. This yield factor includes effects due to manipulation or chemical losses as well as the effects of spreading and self absorption.

1083773

REFERENCES

1. Bureau of Standards Notes, Nucleonics, 2, pp. 84, April, 1948.

2. P. E. Yankwich and J. Weigl, The Relation of Backscattering to Self-absorption. MDDC-1739

3. N. E. Ballow et. al, Absorption and Scattering of Beta Particles and Application to Determination of Disintegration Rates of Radioactive Sources. MDDC-630.

4. B. P. Burtt, The Standardization and Use of Radium E Sources for Absolute Beta Counting. AECU-320.

5. E. Broda, et. al. The Correction for Self-Weakening in Beta Ray Measurements. Proc. Phys. Soc. 60, 460-466, May 1, 1948

6. W. E. Crummitt, J. Gueron, et. al., On the Self-Weakening in Beta Ray Measurements. MC-46, March 17, 1944. (Secret)

7. T. P. Kohman, A General Method for Determining Coincidence Corrections of Counting Instruments. MDDC-905.

8. Modified AC Chamber, Arrangement and Details, Instrument Division Drawings H-4-370, H-4-374, H-4-633, H-4-662 (Amp. Circuit.)

9. Mica Window Assembly, Instrument Division. Drawing, H-4-503.

10. Modified Mica Window Tube Holder.--Arrangement H-4-689; Details, H-4-683.

11. B. B. Cunningham, A. Ghiorso, and J. C. Hindman, Metallurgical Project Report CN-1241 (A-1818) January 5, 1944.

12. P. E. Yankwich Correcting for Absorption of Beta Particles in Thick Samples. A General Method for Use in Tracer Work. CC-R-3567.

13. W. B. Mann and G. B. Parkinson, A Geiger-Mueller Counting Unit and External Quenching Equipment for the Estimation of C^{14} in Carbon Dioxide. Rev. Sci. Inst. 20, 41-47, January, 1949.

1083774

14. G. R. Hennig, Conversion of Carbon Dioxide to Methane for Counting C^{14}. AECD-1794.

15. S. C. Brown and W. W. Miller, Carbon Dioxide Filled Geiger-Mueller Counters. Rev. Sci. Inst. 18, #7; 496-500, July, 1947.

16. Private communication, G. R. Hennig to R. C. Thorburn, June 8, 1950.

1083775